AD_____

Award Number: W81XWH-09-1-0056

TITLE: Investigating the Role of Cyclin D1 in the Promotion of Genomic Instability and Breast Cancer

PRINCIPAL INVESTIGATOR: Lauren L. Pontano
J. Alan Diehl

CONTRACTING ORGANIZATION: University of Pennsylvania
Philadelphia, PA 19104

REPORT DATE: September 2011

TYPE OF REPORT: Annual Summary

PREPARED FOR: U.S. Army Medical Research and Materiel Command
Fort Detrick, Maryland 21702-5012

REPORT DOCUMENTATION PAGE

Form Approved
OMB No. 0704-0188

1. REPORT DATE	2. REPORT TYPE	3. DATES COVERED
September 2011	Annual Summary	15 February 2009 – 14 August 2011

4. TITLE AND SUBTITLE

Investigating the Role of Cyclin D1 in the Promotion of Genomic Instability and Breast Cancer

5a. CONTRACT NUMBER

5b. GRANT NUMBER
W81XWH-09-1-0056

5c. PROGRAM ELEMENT NUMBER

6. AUTHOR(S)

Laura L. Pontano and Dr. J. Alan Diehl

E-Mail: lpvaites@gmail.com

5d. PROJECT NUMBER

5e. TASK NUMBER

5f. WORK UNIT NUMBER

7. PERFORMING ORGANIZATION NAME(S) AND ADDRESS(ES)

University of Pennsylvania
Philadelphia, PA 19104

8. PERFORMING ORGANIZATION REPORT NUMBER

9. SPONSORING / MONITORING AGENCY NAME(S) AND ADDRESS(ES)
U.S. Army Medical Research and Materiel Command
Fort Detrick, Maryland 21702-5012

10. SPONSOR/MONITOR'S ACRONYM(S)

11. SPONSOR/MONITOR'S REPORT NUMBER(S)

12. DISTRIBUTION / AVAILABILITY STATEMENT
Approved for Public Release; Distribution Unlimited

13. SUPPLEMENTARY NOTES

14. ABSTRACT
Cyclin D1 deregulation is implicated in the genesis of breast cancer, and elevated cyclin D1 protein expression occurs in the absence of gene amplification, suggesting that post-translational regulation is disrupted during the neoplastic process. Cyclin D1 protein is tightly regulated following the G1/S transition via threonine-286 (T286) phosphorylation and cytoplasmic degradation directed by the SCFFbx4 E3 ubiquitin ligase. Disruption of this regulation is deleterious to cell homeostasis, as nuclear cyclin D1 accumulation promotes DNA re-replication and genomic instability mediated by CUL4 repression and subsequent stabilization of the replication factor CDT1. Consistently, our recent work utilizing Fbx4-/- primary murine embryonic fibroblasts (MEFs) revealed that loss of Fbx4 accelerates growth, facilitates cyclin D1 protein stabilization in S-phase, and promotes nuclear cyclin D1 accumulation. However, increased proliferation in early passage Fbx4-/- MEFs is antagonized by DNA damage checkpoint activation with marked accumulation of DNA double strand break (DSB)-associated nuclear foci, consistent with nuclear cyclin D1 driving genomic instability. Additionally, further molecular dissection of nuclear cyclin D1-dependent genomic instability identified the protein arginine methyltransferase 5/methylosome protein 50 (PRMT5/MEP50) complex as a substrate and effector of cyclin D1-dependent neoplastic transformation, as nuclear cyclin D1 retention during S-phase increases PRMT5-dependent histone methylation at key target promoters, including CUL4A/B, providing a direct correlation among aberrant cyclin D1/CDK4 activity, transcriptional regulation, and perturbation of DNA replication fidelity. Collectively, these findings reveal an intricate relationship wherein nuclear cyclin D1/CDK4 activity modulates genetic alterations necessary for perturbed DNA replication, genomic instability, and ultimately neoplasia.

15. SUBJECT TERMS
Cyclin D1, cell cycle regulation, DNA replication, DNA damage, SCF ubiquitin ligase (Fbx4)

16. SECURITY CLASSIFICATION OF:			17. LIMITATION OF ABSTRACT	18. NUMBER OF PAGES	19a. NAME OF RESPONSIBLE PERSON
a. REPORT	b. ABSTRACT	c. THIS PAGE			USAMRMC
U	U	U	UU	60	19b. TELEPHONE NUMBER *(include area code)*

Table of Contents

	Page
Introduction……..…….…..	**4**
Research Summary……	**4**
Key Research Accomplishments……..	**6**
Reportable Outcomes……	**7**
Conclusion……	**7**
References……	**8**
Appendix 1 (Revised Statement of Work)…….	**9**
Appendix 2 (Accepted Manuscript 2011, *Molecular and Cellular Biology*)…	**10**
Appendix 3 (Published Manuscript 2010, *Cancer Cell*)……	**49**

Introduction

Cyclin D1 serves as a central mediator of mitogen-dependent G1-phase progression. Growth factor signaling induces cyclin D1 expression, association with CDK4, and nuclear accumulation, where active cyclin D1/CDK4 kinase phosphorylates the retinoblastoma protein, triggering release of E2F transcription factors and subsequent gene expression required for progression into S-phase (8, 11-13, 19). Following the G1/S transition, ubiquitin-mediated proteolysis counters cyclin D1 protein accumulation. Specifically, cyclin D1 undergoes GSK3β-dependent phosphorylation, nuclear export, and subsequent recognition by the $SCF^{Fbx4\text{-}\alpha B\ crystallin}$ E3 ubiquitin ligase within the cytoplasm (3, 9, 14). Cyclin D1 overexpression is a hallmark of various malignancies, including nearly 50% of breast cancers; however, many tumors exhibit elevated cyclin D1 protein without gene amplification, providing evidence that cyclin D1 accumulation may result from post-translational regulation (4, 19). Mutations that disrupt cyclin D1 nuclear export and ubiquitin-mediated proteolysis directly contribute to neoplastic transformation (6, 7, 10, 14-16). Importantly, cyclin D1 mutations resulting in its constitutively nuclear localization are rare; however, recent work identified mutations within the E3 ubiquitin ligase component Fbx4, which result in impaired ligase activity and subsequent cyclin D1 stabilization (6, 7, 16).

Impaired cyclin D1 threonine 286 phosphorylation or Fbx4-dependent degradation is sufficient to promote DNA re-replication and transformation *in vitro* (1, 3, 6) and in mouse models (10, 15). Mechanistic analyses revealed that nuclear cyclin D1 accumulation during S-phase disrupts temporal DNA replication via transcriptional repression of the *CUL4* E3 ubiquitin ligase and subsequent stabilization of its substrate, CDT1, a replication licensing protein. CDT1 stabilization during S-phase is sufficient to promote DNA re-replication, DNA damage checkpoint activation, and genomic instability (1). Additionally, failure to degrade nuclear cyclin D1 compromises the intra-S-phase response to DNA damage, resulting in radio-resistant DNA synthesis (RDS) and chromosomal aberrations (18). Given these findings, our current work sought to delineate the mechanism of nuclear cyclin D1/CDK4-mediated *CUL4* repression. Furthermore, since mutations in cyclin D1 itself are rare in human tumors, we examined whether alterations in the cyclin D1 E3 ubiquitin ligase, SCFFbx4, contribute to cyclin D1 protein stabilization. To determine whether Fbx4 plays a requisite role in regulating cyclin D1 accumulation and cellular transformation, we generated Fbx4-/- murine embryonic fibroblasts (MEFs) and characterized growth kinetics, cyclin D1 accumulation, and genome integrity in these cells.

Research Summary

Revised Statement of Work Approved

Our initial Tasks 1-3 described in the grant proposal were completed and published prior to the first year of funding (manuscript completion/publication was substantially accelerated due to competition in the field). Tasks 1-3 were completed in entirety, published in a first author manuscript in October of 2008 (18). As recommended by the Breast Cancer Program Grant Manager, a revised statement of work was submitted and approved by the Department of Defense. This revision includes tasks to investigate the role of Fbx4 as a putative tumor suppressor and to elucidate the mechanism of constitutively nuclear cyclin D1-driven neoplastic transformation, which will contribute substantially to our understanding of the role this oncogene plays in promoting tumorigenesis, including breast cancer, where nearly 50% of tumors exhibit elevated cyclin D1. Our revised statement of work, entitled "Investigating the role of cyclin D1 in the promotion of genomic instability and neoplastic transformation," is included as Appendix 1. The published and recently accepted work presented in this final report reflects the tasks and hypotheses generated in our revised statement of work.

Genomic instability is a hallmark of human cancer, involved in both initiation and promotion of disease. Cyclin D1 is frequently overexpressed in human tumors (including breast cancer), and aberrant nuclear accumulation of cyclin D1/CDK4 kinase is associated with DNA re-replication, checkpoint activation in pre-malignant tissue, and genomic instability in malignant lesions (1, 10). Additionally, cyclin D1 is rapidly degraded in a GSK3β- and Fbx4-dependent manner following S-phase DNA damage, an event necessary to maintain genome integrity. Considering that GSK3β phosphorylates cyclin D1, triggering its nuclear export (9), and Fbx4, triggering ligase dimerization and activation (6), **the first task outlined in our revised statement of work interrogated whether Fbx4-mediated cyclin D1 ubiquitylation is regulated by DNA damage.**

To address this task, we initially determined whether Fbx4-dependent cyclin D1 ubiquitylation is increased following DNA damage. *In vitro* ubiquitylation assays were performed utilizing Fbx4 ligase purified from NIH 3T3 cells in S-phase in the presence or absence of DNA damage and purified cyclin D1 substrate. Cyclin D1 is

ubiquitylated by Fbx4 ligase purified from S-phase cells, and this signal is significantly increased when the ligase source is purified from cells following DNA damage (data included in an August 2011 *Molecular and Cellular Biology* accepted manuscript, Appendix 2, Figure 5D). We next examined whether Fbx4 phosphorylation, a marker of active SCFFbx4 ligase, increases following DNA damage. Antibodies were previously generated against phosphorylated serine 12 of human Fbx4; lysates prepared from asynchronous, G1, or S-phase cells were precipitated with pS12 Fbx4 antibody and subjected to immunoblot. Fbx4 phosphorylation increases following S-phase DNA damage, with robust concurrent cyclin D1 threonine 286 phosphorylation (Appendix 2, Figure 5C).

Cyclin D1 degradation following the G1/S transition as well as S-phase DNA damage is required to maintain genome integrity. Constitutively nuclear cyclin D1/CDK4 activity disrupts DNA replication fidelity through repression of *CUL4*, triggering stabilization of the replication factor CDT1 and multiple rounds of origin licensing/firing during a single S-phase (1). **Our second task sought to delineate the mechanism of nuclear cyclin D1-dependent DNA re-replication and genomic instability**, *testing our hypothesis that nuclear cyclin D1/CDK4 kinase activity during S-phase modulates gene expression through phosphorylation of histone methylation machinery*. Collectively, the experiments proposed in this task were completed and published as a co-first author *Cancer Cell* manuscript in October 2010 (2), manuscript included as Appendix 3.

Cyclin D1/CDK4 associates with the protein arginine methyltransferase 5/ Methylsome 50 (PRMT5/MEP50) complex, and previous work indicated that the PRMT5/MEP50 complex modulates transcriptional repression through histone methylation (histone H3, arginine 8; histone H4, arginine 3) at target promoter regions (17). Consequently, we assessed whether PRMT5 methyltransferase activity was required for *CUL4* repression. Knockdown of PRMT5 or MEP50 restored *CUL4A* and *CUL4B* mRNA and protein expression in S-phase HeLa cells transfected with constitutively nuclear cyclin D1T286A/CDK4, with a concomitant reduction in Cdt1 levels and histone arginine methylation (Appendix 3, Figure 3E). Consistent with these findings, we observed increased PRMT5 methyltransferase activity in cells expressing cyclin D1T286A/CDK4 compared to wild type cyclin D1/CDK4 (Appendix 3, Figure 3 B and C). Since CDK4 activity is essential for nuclear cyclin D1-dependent *CUL4* repression (1), we examined whether PRMT5 or MEP50 was phosphorylated by cyclin D1/CDK4 kinase. PRMT5 was not directly phosphorylated by cyclin D1/CDK4; however, consistent with MEP50 being a direct substrate, recombinant MEP50 was phosphorylated by cyclin D1/CDK4 and cyclin D1T286A/CDK4 (Appendix 3, Figure 4). To identify phosphorylation sites, we phosphorylated recombinant MEP50 *in vitro* with purified cyclin D1T286A/CDK4 and subjected it to mass spectrometry, yielding threonine 5 as the phosphorylation site. Alanine substitution of MEP50 threonine 5 dramatically attenuated MEP50 phosphorylation by cyclin D1T286A/CDK4, and subsequent analyses revealed that MEP50 phosphorylation increases intrinsic PRMT5 methyltransferase activity in coupled kinase-methyltransferase reactions (Appendix 3, Figure 4C and D).

We next determined whether PRMT5 mediates cyclin D1T286A-driven transformation by knockdown of PRMT5 in murine fibroblasts, concurrent with expression of oncogenic RasV12 and cyclin D1T286A. While co-expression of cyclin D1T286A and RasV12 induces focus formation in cells treated with control siRNA, knockdown of PRMT5 dramatically reduced focus formation, and consistent with these findings, knockdown of PRMT5 substantially attenuated DNA re-replication in cells expressing cyclin D1T286A/CDK4 (Appendix 3, Figure 6). This data highlights a novel transcriptional regulatory program activated in cells harboring constitutively nuclear cyclin D1, ultimately resulting in neoplastic transformation. Future efforts to determine global gene expression signatures altered through cyclin D1-dependent regulation of PRMT5 involved in neoplastic growth will expand our mechanistic knowledge of the cyclin D1 oncogene.

Since cyclin D1 mutations resulting in constitutively nuclear accumulation are rare in human cancer and inactivating mutations have been identified in Fbx4, **the third task in our revised statement of work focused on determining whether genetic Fbx4 deletion drives nuclear cyclin D1 accumulation and neoplasia** (manuscript accepted for publication at *Molecular and Cellular Biology*, August 26, 2011; accepted version included as Appendix 2)**.** *We hypothesized that cyclin D1 will accumulate in the nucleus of Fbx4-/- MEFs* (murine embryonic fibroblasts)*, promoting increased cell proliferation and transformation in vitro.* Our analyses revealed that cyclin D1 does, in fact, accumulate in the nucleus of early passage Fbx4-/- MEFs, and Fbx4 loss accelerates cell proliferation in early passage MEFs (Appendix 2, Figure 3). However, the initial proliferative advantage observed in early passage Fbx4-/- MEFs is antagonized dramatically by passage 6-7, compared to gradual onset of senescence observed in wild type MEFs cultured on a 3T9 passage protocol. Consequently, we evaluated whether markers of cell cycle arrest were observed in Fbx4-/- MEFs prior to declined proliferation. Importantly, Fbx4-/- MEFs exhibit a marked increase in p53 levels and accumulation of the p53 downstream target p21,

coincident with accumulation of γH2AX, suggesting that DNA damage may promote cell cycle arrest in Fbx4-/- cells (Appendix 2, Figure 4). Consistent with our hypothesis that loss of Fbx4 facilitates nuclear cyclin D1 accumulation, thereby leading to *Cul4* repression and Cdt1 stabilization, Fbx4-/- cells retain Cdt1 in S-phase, with a concomitant reduction in Cul4A. Furthermore, Fbx4-/- cells pulsed with hydroxyurea (HU) during S-phase exhibited a significant increase in metaphase chromosome alterations (Appendix 2, Figure 5A, 4G, respectively).

Given that Fbx4-/- cells accumulate DNA damage and chromosome alterations, we postulated that primary Fbx4-/- MEFs would selectively undergo transformation following expression of oncogenic Ras, while wild type MEFs would undergo oncogene-induced senescence. To test this possibility, we transfected early passage wild type and Fbx4-/- MEFs with empty puromycin vector (Puro) or RasV12 constructs (Ras) and assessed foci formation. Strikingly, loss of one copy (heterozygous, HET) or both copies of Fbx4 (Fbx4-/-, NULL) facilitates oncogenic Ras-mediated cellular transformation *in vitro* (Appendix 2, Figure 6). Importantly, this transformation phenotype is dependent upon cyclin D1/CDK4 function, as dominant negative cyclin D1T156A or kinase deficient CDK4K35M expression attenuates foci formation in the absence of Fbx4. Finally, our recent work revealed that immortalized Fbx4-/- cells undergo spontaneous transformation independent of secondary oncogene expression (Appendix 2, Figure 6), analogous to the cyclin D1T286A mutant (3).

Key Research Accomplishments

1. Contributed to research article published in *Oncogene* assessing cyclin D1 ubiquitylation (5).
    - Confirmed that cyclin D1 degradation following DNA damage requires ubiquitylation of lysine 269.
2. Oral Presentation: 2009 Biomedical Graduate Studies Cell and Molecular Biology Symposium
    - Invited speaker representing the Cancer Biology Program, November 9, 2009.
    - Title of talk: "*Keeping Cyclin D1 in Check*: Role of Fbx4-dependent ubiquitylation in maintaining cell cycle control and genome stability."
3. Invited student attendee at the first annual TMEN (Tumor Micro-Environment Network) Junior Investigator Conference, May 17-19 2010, NY, NY.
    - Recommended by TMEN member Dr. Anil Rustgi for attendance.
    - Participated in discussion sessions and attended various presentations on topics related to *in vivo* models and imaging, tumor progression and metastasis.
4. Oral Presentation: 2010 Annual Department of Cancer Biology Retreat, June 4-6, Cambridge, MD.
    - Selected student speaker.
    - Title of talk: "Mechanism of cyclin D1-dependent genomic instability and neoplastic transformation."
5. Oral Presentation: 2010 Models and Mechanisms of Cancer Meeting, Cold Spring Harbor Laboratories.
    - Selected for oral presentation at this national conference, August 17-21, 2010.
    - Title of talk: "Mechanism of cyclin D1-dependent genomic instability and neoplastic transformation."
6. Publication of a co-first author research article in *Cancer Cell* providing novel insight into the mechanism of nuclear cyclin D1-driven neoplastic transformation (2).
    - Demonstrated that the PRMT5/MEP50 methyltransferase forms a complex with cyclin D1/CDK4.
    - Demonstrated that PRMT5/MEP50 methyltransferase activity was required for nuclear cyclin D1-dependnent *CUL4* repression and subsequent CDT1 stabilization during S-phase.
    - Identified a novel site on MEP50 (threonine 5) that is phosphorylated by cyclin D1/CDK4, and that phosphorylation of this residue promotes increased methyltransferase activity.
    - Demonstrated that PRMT5/MEP50 methyltransferase activity is necessary for nuclear cyclin D1-driven DNA re-replication during S-phase and neoplastic transformation *in vitro*.

7. Oral Presentation: 2011 Ubiquitin Family Meeting, Cold Spring Harbor Laboratories.
    - Selected for oral presentation at this national conference, May 17-21, 2011.
    - Title of talk: “Mechanism of cyclin D1-dependent genomic instability and neoplastic transformation.”
8. Accepted first author manuscript for publication at *Molecular and Cellular Biology*, investigating the role of Fbx4 in regulating cyclin D1 accumulation and preventing neoplastic transformation.
    - Manuscript title: “The Fbx4 tumor suppressor regulates Cyclin D1 accumulation and prevents neoplastic transformation.”
    - Demonstrated that Fbx4-/- primary murine embryonic fibroblasts (MEFs) exhibit cyclin D1 stabilization and increased rate of proliferation compared to wild type MEFs.
    - Demonstrated that the initial proliferative advantage in Fbx4-/- primary MEFs is antagonized by DNA damage checkpoint activation and growth arrest at later passages.
    - Demonstrated that loss of Fbx4 in primary MEFs synergizes with Ras expression to mediate neoplastic transformation *in vitro*.
9. Poster Presentation: 2011 Era of Hope Conference, August 2-5, 2011.
    - Poster competition finalist.
    - Title of poster: “Mechanism of cyclin D1-dependent genomic instability and neoplastic transformation.”

Reportable Outcomes

Aggarwal P*, **Pontano Vaites L***, Kim JK, Mellert H, Gurung B, Nakagawa H, Herlyn M, Hua X, Rustgi AK, McMahon SB, and Diehl JA. Nuclear cyclin D1/CDK4 kinase regulates *CUL4* expression and triggers neoplastic growth via activation of the PRMT5 methyltransferase. (2010). *Cancer Cell* 18: 329-340.
***These authors contributed equally to this work.**

Pontano Vaites L, Lee EK, Lian Z, Barbash O, Roy D, Wasik M, Klein-Szanto AJP, Rustgi AK, and Diehl JA. The Fbx4 tumor suppressor regulates cyclin D1 accumulation and prevents neoplastic transformation. (2011). *MCB* doi:10.1128/MCB.05733-11.

Conclusion

Collectively, our data reveal that failure to degrade cyclin D1 following the G1/S transition results in nuclear accumulation of active cyclin D1/CDK4 kinase and transcriptional regulation that facilitates neoplastic growth. This work supports a model wherein Fbx4-mediated cyclin D1 degradation is essential to maintain genome integrity and cell homeostasis. Our functional analyses demonstrated that PRMT5 methyltransferase activity is necessary for nuclear cyclin D1-driven cell transformation, suggesting that the PRMT5 methyltransferase may be a suitable therapeutic target for tumors exhibiting cyclin D1 overexpression. Furthermore, interrogation of the Fbx4-dependent cyclin D1 degradation pathway suggests that Fbx4 functions as a tumor suppressor, preventing cyclin D1 nuclear accumulation and oncogenic function following the G1/S transition. Ultimately, these findings redefine the role of cyclin D1 as an oncogene; not only does overexpression drive cellular proliferation, but sustained nuclear accumulation results in genetic alterations necessary for perturbed DNA replication, genomic instability, and finally, tumorigenesis.

References

1. **Aggarwal, P., M. D. Lessie, D. I. Lin, L. Pontano, A. B. Gladden, B. Nuskey, A. Goradia, M. A. Wasik, A. J. Klein-Szanto, A. K. Rustgi, C. H. Bassing, and J. A. Diehl.** 2007. Nuclear accumulation of cyclin D1 during S phase inhibits Cul4-dependent Cdt1 proteolysis and triggers p53-dependent DNA rereplication. Genes Dev **21:**2908-22.
2. **Aggarwal, P., L. P. Vaites, J. K. Kim, H. Mellert, B. Gurung, H. Nakagawa, M. Herlyn, X. Hua, A. K. Rustgi, S. B. McMahon, and J. A. Diehl.** Nuclear cyclin D1/CDK4 kinase regulates CUL4 expression and triggers neoplastic growth via activation of the PRMT5 methyltransferase. Cancer Cell **18:**329-40.
3. **Alt, J. R., J. L. Cleveland, M. Hannink, and J. A. Diehl.** 2000. Phosphorylation-dependent regulation of cyclin D1 nuclear export and cyclin D1-dependent cellular transformation. Genes Dev **14:**3102-14.
4. **Arnold, A., and A. Papanikolaou.** 2005. Cyclin D1 in breast cancer pathogenesis. J Clin Oncol **23:**4215-24.
5. **Barbash, O., E. Egan, L. L. Pontano, J. Kosak, and J. A. Diehl.** 2009. Lysine 269 is essential for cyclin D1 ubiquitylation by the SCF(Fbx4/alphaB-crystallin) ligase and subsequent proteasome-dependent degradation. Oncogene **28:**4317-25.
6. **Barbash, O., P. Zamfirova, D. I. Lin, X. Chen, K. Yang, H. Nakagawa, F. Lu, A. K. Rustgi, and J. A. Diehl.** 2008. Mutations in Fbx4 Inhibit Dimerization of the SCF(Fbx4) Ligase and Contribute to Cyclin D1 Overexpression in Human Cancer. Cancer Cell **14:**68-78.
7. **Benzeno, S., F. Lu, M. Guo, O. Barbash, F. Zhang, J. G. Herman, P. S. Klein, A. Rustgi, and J. A. Diehl.** 2006. Identification of mutations that disrupt phosphorylation-dependent nuclear export of cyclin D1. Oncogene **25:**6291-303.
8. **Calbo, J., M. Parreno, E. Sotillo, T. Yong, A. Mazo, J. Garriga, and X. Grana.** 2002. G1 cyclin/cyclin-dependent kinase-coordinated phosphorylation of endogenous pocket proteins differentially regulates their interactions with E2F4 and E2F1 and gene expression. J Biol Chem **277:**50263-74.
9. **Diehl, J. A., M. Cheng, M. F. Roussel, and C. J. Sherr.** 1998. Glycogen synthase kinase-3beta regulates cyclin D1 proteolysis and subcellular localization. Genes Dev **12:**3499-511.
10. **Gladden AB, W. R., Aggarwal P, Wasik MA, Diehl JA** 2006. Expression of constitutively nuclear cyclin D1 in murine lymphocytes induces B-cell lymphoma Oncogene **25:**998-1007.
11. **Harbour, J. W., R. X. Luo, A. Dei Santi, A. A. Postigo, and D. C. Dean.** 1999. Cdk phosphorylation triggers sequential intramolecular interactions that progressively block Rb functions as cells move through G1. Cell **98:**859-69.
12. **Hatakeyama, M., J. A. Brill, G. R. Fink, and R. A. Weinberg.** 1994. Collaboration of G1 cyclins in the functional inactivation of the retinoblastoma protein. Genes Dev **8:**1759-71.
13. **Leng, X., M. Noble, P. D. Adams, J. Qin, and J. W. Harper.** 2002. Reversal of growth suppression by p107 via direct phosphorylation by cyclin D1/cyclin-dependent kinase 4. Mol Cell Biol **22:**2242-54.
14. **Lin, D. I., O. Barbash, K. G. Kumar, J. D. Weber, J. W. Harper, A. J. Klein-Szanto, A. Rustgi, S. Y. Fuchs, and J. A. Diehl.** 2006. Phosphorylation-dependent ubiquitination of cyclin D1 by the SCF(FBX4-alphaB crystallin) complex. Mol Cell **24:**355-66.
15. **Lin, D. I., M. D. Lessie, A. B. Gladden, C. H. Bassing, K. U. Wagner, and J. A. Diehl.** 2007. Disruption of cyclin D1 nuclear export and proteolysis accelerates mammary carcinogenesis. Oncogene.
16. **Moreno-Bueno, G., S. Rodriguez-Perales, C. Sanchez-Estevez, D. Hardisson, D. Sarrio, J. Prat, J. C. Cigudosa, X. Matias-Guiu, and J. Palacios.** 2003. Cyclin D1 gene (CCND1) mutations in endometrial cancer. Oncogene **22:**6115-8.
17. **Pal, S., S. N. Vishwanath, H. Erdjument-Bromage, P. Tempst, and S. Sif.** 2004. Human SWI/SNF-associated PRMT5 methylates histone H3 arginine 8 and negatively regulates expression of ST7 and NM23 tumor suppressor genes. Mol Cell Biol **24:**9630-45.
18. **Pontano, L. L., P. Aggarwal, O. Barbash, E. J. Brown, C. H. Bassing, and J. A. Diehl.** 2008. Genotoxic stress-induced cyclin D1 phosphorylation and proteolysis are required for genomic stability. Mol Cell Biol **28:**7245-58.
19. **Sherr, C. J.** 1996. Cancer cell cycles. Science **274:**1672-7.

Appendices

Pontano, Laura L.

Revised Statement of Work

Investigating the role of cyclin D1 in the promotion of genomic instability and neoplastic transformation

Task 1. Determine whether Fbx4-mediated cyclin D1 ubiquitylation is regulated by DNA damage (Months 1-6).

a. Determine whether GSK3β-dependent Fbx4 phosphorylation increases following S-phase DNA damage (Months 1-2).
b. Determine whether Fbx4-dependent ubiquitin ligase activity increases following DNA damage (Months 3-6).

Task 2. Delineate the mechanism of nuclear cyclin D1-dependent DNA re-replication and genomic instability (Months 6-20).

a. Assess whether PRMT5 methyltransferase activity is required for *Cul4* repression in the presence of constitutively nuclear cyclin D1 during S-phase (Months 6-10).
b. Determine whether cyclin D1/CDK4 kinase phosphorylates PRMT5/MEP50 methyltransferase components (Months 10-14).
c. Determine whether PRMT5 methyltransferase activity is necessary to promote nuclear cyclin D1-driven DNA re-replication and cellular transformation (Months 14-20).

Task 3. Determine whether genetic Fbx4 deletion drives nuclear cyclin D1 accumlulation and neoplastic transformation (Months 10-30).

a. Evaluate nuclear cyclin D1 accumulation in Fbx4-deficient murine embryonic fibroblasts (MEFs) (Months 10-14).
b. Determine whether Fbx4 loss alters cell proliferation and onset of senescence in primary MEFs (Months 14-20).
c. Assess accumulation of DNA damage in early passage Fbx4-deficient primary MEFs (Months 18-24).
d. Determine whether loss of Fbx4 promotes cellular transformation *in vitro* (Months 24-30).

The Fbx4 Tumor Suppressor Regulates Cyclin D1 Accumulation and Prevents Neoplastic Transformation

Laura Pontano Vaites[1,2], Eric K. Lee[1,2], Zhaorui Lian[1,2], Olena Barbash[1,2], Darshan Roy[3], Mariusz Wasik[3], Andres J.P. Klein-Szanto[4], Anil K. Rustgi[5,6,7,8], and J. Alan Diehl[1,2,8,*]

[1]The Leonard and Madlyn Abramson Family Cancer Research Institute; [2]Department of Cancer Biology; [3]Department of Pathology and Laboratory Medicine, University of Pennsylvania, Philadelphia, PA 19104, USA; [4]Histopathology Facility, Fox Chase Cancer Center, Philadelphia, PA 19111, USA; [5]Division of Gastroenterology; [6]Department of Medicine; [7]Department of Genetics; [8]Abramson Cancer Center, University of Pennsylvania, Philadelphia, PA 19104, USA.

Running Title: Fbx4 is a *bona fide* tumor suppressor.

Key words: SCF^{Fbx4}/Ubiquitin ligase/Cyclin D1/Tumor Suppressor/Neoplasia

Word count Abstract: 191

Word count Materials and Methods: 1,283

Word count Intro, Results, Discussion, Figure Legends: 5,012

[*] To whom correspondence should be directed: adiehl@mail.med.upenn.edu

454 BRB II/III

421 Curie Boulevard

Philadelphia, PA 19104

Phone: (215)746-6389; Fax: (215)746-5511

ABSTRACT

SCF E3 ubiquitin ligase complexes modulate the accumulation of key cell cycle regulatory proteins. Following the G1/S transition, SCF^{Fbx4} targets cyclin D1 for proteasomal degradation, a critical event necessary for DNA replication fidelity. Deregulated cyclin D1 drives tumorigenesis, and inactivating mutations in Fbx4 have been identified in human cancer, suggesting that Fbx4 may function as a tumor suppressor. $Fbx4^{+/-}$ and $Fbx4^{-/-}$ mice succumb to multiple tumor phenotypes including lymphomas, histiocytic sarcomas, and less frequently, mammary and hepatocellular carcinomas. Tumors and pre-malignant tissue from $Fbx4^{+/-}$ and $Fbx4^{-/-}$ mice exhibit elevated cyclin D1, consistent with cyclin D1 as a target of Fbx4. Molecular dissection of the Fbx4 regulatory network in murine embryonic fibroblasts (MEFs) revealed that loss of Fbx4 results in cyclin D1 stabilization and nuclear accumulation throughout cell division. Increased proliferation in early passage primary MEFs is antagonized by DNA damage checkpoint activation, consistent with nuclear cyclin D1-driven genomic instability. Furthermore, $Fbx4^{-/-}$ MEFs exhibited increased susceptibility to Ras-dependent transformation *in vitro*, analogous to tumorigenesis observed in mice. Collectively, these data reveal a requisite role for the SCF^{Fbx4} E3 ubiquitin ligase in regulating cyclin D1 accumulation, consistent with tumor suppressive function *in vivo*.

INTRODUCTION

Cell cycle progression is intricately controlled by coordinated expression and ubiquitin-dependent degradation of key regulatory proteins. Ubiquitylation of target substrates requires the concerted activity of an Ub-activating enzyme (E1), recruitment of an Ub-conjugating enzyme (E2), and an E3 ubiquitin ligase. Although some E3 ubiquitin ligases directly mediate transfer of ubiquitin, for example the HECT-domain family of E3 ligases, many E3 ligases function as multi-subunit complexes that bridge the charged E2 enzyme with a given substrate (20). The Skp1-Cul1-F-box (SCF) family of E3 ubiquitin ligases is an example of the latter and promotes polyubiquitylation of mainly phosphorylated substrates, including G1/S regulatory proteins (11, 12, 27, 32, 43). Specificity of SCF ligases is conferred by the F-box protein, which bridges substrate molecules with the core ligase machinery. F-box proteins contain a conserved F-box domain, required for Skp1 binding and recruitment of core ligase components Cul1, Rbx1, and E2, as well as a substrate-recognition domain within the C-terminus (39, 43, 51).

The F-box protein, Fbx4, regulates ubiquitylation of cyclin D1 following the G1/S transition (32). Similar to Fbw7, an ubiquitin ligase for targets such as cyclin E, c-Myc, and Notch (27, 47-50, 54, 55), and β-TrCP, an E3 ligase for targets including IκB, β-catenin, Cdc25A, and Emi1 (10, 16, 18, 24, 26, 28, 36, 38, 45, 46, 52). Fbx4 undergoes dimerization; however, in contrast to either Fbw7 or β-TrCP, Fbx4 dimerization occurs in a cell cycle-dependent manner (5, 17, 44, 46). Fbx4 dimerization requires GSK3β-dependent phosphorylation at serine 12, which triggers ligase activation at the G1/S transition (5, 32). Critically, mutations that stabilize cyclin D1 and thereby trigger nuclear accumulation of active cyclin D1/CDK4 drive cell transformation (1-3). While cyclin D1 overexpression occurs in multiple human malignancies (4, 6-8, 14, 19, 21-23, 25), overexpression of wild type cyclin D1 in an Fbx4-proficient system is insufficient to drive

spontaneous transformation (3, 5), supporting a model wherein cytoplasmic recognition of phosphorylated cyclin D1 by Fbx4 is sufficient to maintain cellular integrity.

Cyclin D1 mutations that impede degradation and trigger nuclear accumulation promote neoplastic growth (1, 3, 5, 9, 35, 37); however such mutations are rare in human cancer. Recent work identified inactivating Fbx4 mutations in human cancers that impair ligase phosphorylation, and dimerization. Such tumors exhibit marked cyclin D1 nuclear accumulation, highlighting a novel mechanism for cyclin D1 deregulation in cancer (5). Taken together, these findings suggest that Fbx4 is tumor suppressor, preventing aberrant cyclin D1 accumulation.

To investigate the tumor suppressor function of Fbx4, we ablated the murine *Fbx4* gene. $Fbx4^{-/-}$ mice are viable and lack major developmental defects. However, $Fbx4^{-/-}$ MEFs exhibit cyclin D1 stabilization and subsequent nuclear localization, with concomitant induction of DNA damage, consistent with a model wherein nuclear cyclin D1/CDK4 kinase drives genomic instability. Finally, Fbx4 deficiency facilitates cellular transformation *in vitro*, and both $Fbx4^{+/-}$ and $Fbx4^{-/-}$ mice succumb to multiple tumor phenotypes *in vivo* with a marked increase in cyclin D1 level, supporting the notion that Fbx4 is a *bona fide* tumor suppressor.

MATERIALS AND METHODS

Targeting Vector Construction and Generation of Fbx4$^{-/-}$ Mice—The engineered construct targeting murine *Fbx4* exon 2 was developed by Vega Biolab (Philadelphia, PA). The targeting vector was electroporated into ES cells, and clones harboring a correctly targeted allele with a normal karyotype were injected in B6 blastocysts by the University of Pennsylvania core facility for generation of chimeric mice with germline transmission; these mice were intercrossed with EIIa-Cre transgenic mice to generate Fbx4 heterozygous progeny. Genotypes were verified by PCR using tail DNA. Extraction and PCR were performed with Extract-N-Amp Tissue PCR Kit (Sigma-Aldrich). Genotyping primers are as follows:

1loxP Forward: 5'-GGCAGAGCTTGAGTTTGCAACATTTCAGGTG-3', and

3loxP Reverse: 5'-TCCTGATCTTTGGAAATTCTTCCTCTGAGT-3'.

Aged mice were monitored closely for signs of distress or palpable tumor mass according to IACUC guidelines, and event-free survival was assessed by Kaplan-Meier analysis.

Southern blot analysis—5' and 3' probes in the genomic region flanking *Fbx4* exon 1-3 (site of homologous recombination, see Fig. 1) were generated. The 5' probe generates a band of 15kb for normal *Fbx4* locus, and a 10kb band for an allele that has undergone homologous recombination.

Histology/Immunohistochemistry (IHC)—Tissues were fixed in 10% buffered formalin overnight, followed by dehydration in a series of ethanol and paraffin embedding and sectioning. Antibodies utilized for IHC staining were purified cyclin D1 (72-13G, Santa Cruz), Ki-67 (Novocastra), phospho-ATM (Millipore), and γH2AX (Millipore).

MEFs and Cell Culture—Mouse embryos extracted at day 14 of gestation were maintained on a 3T9 passage protocol, cultured in DMEM containing 10% fetal bovine serum, 2mM glutamine, 0.1mM non-essential amino acids, 55μM β-mercaptoethanol, and 10μg/mL gentamicin. For growth curves, $1x10^5$ cells were plated on 35mm dishes in duplicate and counted every 24 hours by using a hemocytometer. Primary MEFs were immortalized by lentiviral infection with $p19^{Arf}$ shRNA vector. Immortalized cells and NIH3T3 fibroblasts were cultured in complete DMEM containing 10% fetal bovine serum, glutamine, and 1% penicillin/streptomycin. Cell synchronization was achieved by serum starvation for 24-48 hours, followed by serum stimulation to allow cell cycle entry.

Western analysis and Immunoprecipitation—Whole tissues and cultured cells were lysed in Tween-20 buffer containing 50mM HEPES (pH 8.0), 150mM NaCl, 2.5mM EGTA, 1mM EDTA, 0.1% Tween-20, and protease/phosphatase inhibitors (1mM PMSF, 20U/mL aprotinin, 5mg/mL leupeptin, 1mM DTT, 0.4mM NaF, and 10mM β-glycerophosphate). Whole tissues were homogenized in Tween-20 buffer with inhibitors, and lysates were sonicated prior to clearing by centrifugation at 4°C for 30 minutes. Lysate protein concentration was determined by BCA assay, and proteins were resolved by SDS-PAGE, transferred to nitrocellulose membranes, and subjected to immunoblotting. Antibodies utilized include Fbx4 rabbit polyclonal antibodies (YenZym, Rockland Immunochemicals), cyclin D1 mouse monoclonal D1-72-13G, H4R3 (Abcam), γH2AX (Cell Signaling), p53 mouse monoclonal pab421, p21 and cyclin A (Santa Cruz), phosphorylated threonine 286 cyclin D1 antibody (pT286 Cyc D1) and phosphorylated serine 12 Fbx4 antibody (pS12 Fbx4, Yenzym), $p19^{Arf}$ (Abcam), $p16^{Ink4a}$ (Santa Cruz), Cul4a (Bethyl), Cdt1 (Santa Cruz), Chk2 (BD Biosciences), total and cleaved Caspase 3 (Cell Signaling), and β-Actin (Sigma). For cyclin D1 immune precipitation experiments, cells were lysed in Tween-20 buffer, and 1mg of total protein was immune precipitated with cyclin D1 72-13G antisera for 1 hour at 4°C.

Immunofluorescence—Primary MEFs were plated at optimal densities on glass coverslips. For cyclin D1 localization, passage 3 primary MEFs were grown to 70-80% density, then fixed in 1:1 methanol:acetone for 10 minutes at -20°C. Coverslips were dried then rehydrated with PBS, blocked with 10% fetal calf serum in PBS, then incubated with cyclin D1 primary antibody for 1 hour. Coverslips were washed with PBS, followed by incubation with anti-mouse Alexa Fluor 546 secondary antibody for 30 minutes. Coverslips were washed with PBS, dried by 70% and 100% ethanol washes and mounted with Vectashield containing DAPI (Vector Laboratories). For γH2AX foci visualization, passage 3 cells maintained under atmospheric (21%) oxygen conditions or physiological (3%) oxygen tension were plated on glass coverslips at a density of $1x10^5$ cells/well of a 6-well plate and cultured for 24 hours. Cells were fixed and blocked as described above, followed by incubation with γH2AX antibodies for 2 hours. Coverslips were washed with PBS, then incubated with anti-rabbit Alexa Fluor 488 secondary antibody for 30 minutes. Coverslips were mounted as described above and visualized with a Nikon Eclipse 80*i* fluorescent microscope.

In vivo Ubiquitylation—Immortalized MEFs were synchronized by serum starvation and stimulated for 15 hours to enter early S-phase. Cells were treated for 3 hours with 10μM MG132 (Calbiochem) for proteasome inhibition and harvested in Tween 20 buffer containing proteasome and phosphatase inhibitors, 1mM DTT, 10mM N-ethylmaleimide (NEM), and 20μM MG132, followed by immune precipitation with cyclin D1 72-13G antibody as described above. Immune precipitation samples were resolved by SDS-PAGE on 10% poly-acrylamide gels and immunoblotted with phospho-cyclin D1 T286 antibodies and total ubiquitin antibodies to visualize ubiquitylated cyclin D1 laddering.

In vitro Ubiquitylation—NIH 3T3 cells were synchronized by serum starvation, followed by serum stimulation to enter S-phase. Cells were either untreated or subjected to 10Gy γIR, followed by 30 minutes of recovery. Cells were then harvested in Tween-20 buffer, and 1mg of total protein was immune precipitated with Fbx4-specific antibody and protein A sepharose beads for 4 hours at 4°C. Fbx4-containing endogenous SCF complexes were washed 4x with Tween-20 buffer, then 3x with kinase buffer (20mM Tris, 40mM $MgCl_2$, 2.5mM EGTA). Beads containing SCF^{Fbx4} complexes were then mixed with Sf9-produced purified cyclin D1 substrate, ATP, ubiquitin, E1, E2, MG132, ubiquitin aldehyde, okadaic acid, energy regeneration buffer (20x: 10mM ATP, 20mM Hepes pH 7.4, 10mM MgOAc, 300mM creatine phosphate, 0.5mg/mL creatine phosphokinase) and kinase buffer to a final volume of 50μL. Reactions were carried out at 37°C for 30 minutes, followed by SDS-PAGE for visualization of ubiquitylated cyclin D1 by western blot.

Metaphase Spreads—Immortalized MEFs were synchronized by serum starvation, followed by serum stimulation to allow progression into S-phase. Cells in mid-S-phase were pulsed with HU for 2 hours, followed by HU washout and incubation in complete DMEM media. Cells were arrested in metaphase by treatment with colcemid for 2 hours, harvested, treated with hypotonic KCl solution and fixed with methanol-acetic acid. Metaphase spreads were dropped onto glass slides and permitted to dry, followed by Giemsa staining (Sigma). The average number of chromatid breaks per cell was scored in two independent biological replicate cell lines for each genotype. For normal lymphocyte or lymphoma cell metaphase spreads, single cell suspensions of splenic or mesenteric node B-cells were prepared, pulsed with HU for 2 hours to induce replication stress, followed by HU washout and incubation with colcemid for 2 hours to arrest cells in metaphase. Metaphase spreads were dropped and analyzed as described for MEF cells above.

In vitro Transformation Assays—Primary passage 3 MEFs were transduced with pBabe-Puro (empty vector) or pBabe-RasV12 retrovirus. 24 hours post infection, cells were trypsinized and re-plated at a density of $1.5x10^5$ cells/35mm plate in duplicate. Cells were cultured in DMEM containing 5% serum, with media changed every 2 days for 21 days, followed by giemsa stain to visualize foci. To assess cyclin D1-dependence, primary passage 4 MEFs were transfected with pBabe-Puro empty vector, pBabe-RasV12, kinase deficient pSRα-CDK4(K35M), or dominant negative pBabe-cyclin D1T156A. 24 hours post transfection, cells were trypsinized and plated as described above. Additionally, early passage spontaneously immortalized cells were transfected with the aforementioned constructs, and plated and grown as described above. For spontaneous transformation of p19shRNA-immortalized MEFs, cells were plated at a density of $1.5x10^5$/35mm plate and cultured as described above.

Statistical analysis—Prism GraphPad Software was utilized for generating Kaplan-Meier mouse event-free survival plots and statistical analysis of survival and tumor onset. All other statistical analyses utilized a two-tailed student's t-test, with p-values less than 0.05 indicating statistical significance. Error bars represent the mean ± the standard deviation.

RESULTS

Generation of Fbx4$^{+/-}$ and Fbx4$^{-/-}$ mice

To directly assess the tumor suppressor function of Fbx4 we generated a targeting vector to facilitate deletion of murine *Fbx4* by homologous recombination in embryonic stem (ES) cells. LoxP sites were inserted flanking exon 2, with a downstream neomycin (Neo) cassette flanked by a third LoxP site. Cre-mediated recombination and deletion of exon 2 removes F-box sequences critical for Skp1 recruitment and assembly of a functional ligase, resulting in a frameshift and premature termination (Fig. 1A). The targeting construct was electroporated into ES cells, and correctly targeted clones were identified by Southern hybridization (Fig. 1B). ES cell clones harboring a correctly targeted allele with a normal karyotype were injected in C57BL/6 blastocysts; two clones resulted in germline transmission. Chimeric mice were intercrossed with EIIa-Cre transgenic mice to generate Fbx4 heterozygous progeny (genotype confirmation, Fig. 1C). Both Fbx4$^{+/-}$ and Fbx4$^{-/-}$ animals are viable and fertile, with no apparent developmental defects.

Multiple tissues harvested from young (1-2 month old) animals were assessed for cyclin D1 and Fbx4 expression. Importantly no Fbx4 protein could be detected from the knockout allele using both N- and C-terminal Fbx4-specific antibodies (data not shown), suggesting that deletion of exon 2 creates an inherently unstable protein that is rapidly degraded. Among the tissues examined, cyclin D1 protein accumulation was noted in the mammary gland, lung, thymus and spleen (Fig. 2A-D). Increased cyclin D1 accumulation was also observed in both Fbx4$^{+/-}$ and Fbx4$^{-/-}$ primary MEFs (Fig. 2E). RT-PCR analysis revealed equivalent levels of cyclin D1 message in Fbx4$^{+/+}$, Fbx4$^{+/-}$, and Fbx4$^{-/-}$ MEFs, suggesting that protein accumulation occurs at the post-translational level (Fig. 2F).

Fbx4 deletion promotes cyclin D1 stabilization and nuclear accumulation

To dissect the molecular mechanism underlying cyclin D1 accumulation in $Fbx4^{+/-}$ and $Fbx4^{-/-}$ mice, we prepared MEFs from d14 embryos and examined cell proliferation and cyclin D1 stability. Primary $Fbx4^{+/-}$ and $Fbx4^{-/-}$ MEFs exhibit cyclin D1 stabilization in S-phase, with increased cyclin D1 half-life (Fig. 3A). Importantly, cyclin D1 stabilization correlates with its robust nuclear accumulation at the expense of cytoplasmic staining in primary MEFs (Fig. 3B). Consistent with cyclin D1 deregulation in the absence of Fbx4, early passage primary MEFs also exhibit an increased rate of proliferation compared to wild type MEFs (Fig. 3C). Subsequently, we determined whether cyclin D1 protein is stabilized throughout S-phase in $Fbx4^{-/-}$ cells. MEFs were immortalized with $p19^{Arf}$ shRNA, allowing extended culture and effective synchronization, and cyclin D1 levels were assessed across late G1 through mid S-phase. In $Fbx4^{+/+}$ cells, cyclin D1 is rapidly degraded following the G1/S transition; conversely, cyclin D1 protein is elevated, reflecting increased stability, in $Fbx4^{-/-}$ cells (Fig. 3D). Furthermore, threonine 286 phosphorylated (pT286) cyclin D1 accumulates in $Fbx4^{-/-}$ cells, consistent with reduced degradation (Fig. 3E). We also determined whether cyclin D1 S-phase ubiquitylation requires Fbx4. Wild type and null cells were synchronized and stimulated to enter S-phase with serum-derived growth factors; cells were treated with the proteasome inhibitor MG132 to allow accumulation of poly-ubiquitylated proteins, and cyclin D1 was immunopurified. Immunoblot revealed reduced cyclin D1 polyubiquitylation in $Fbx4^{-/-}$ cells compared to $Fbx4^{+/+}$ controls, suggesting that impaired cyclin D1 ubiquitylation/degradation drives nuclear cyclin D1 accumulation in $Fbx4^{-/-}$ cells (Fig. 3F).

Enhanced proliferation is antagonized by DNA damage in $Fbx4^{-/-}$ MEFs

MEFs were maintained on a 3T9 passage protocol to evaluate the onset of cellular senescence. While early passage $Fbx4^{-/-}$ MEFs initially accumulate to a higher density, proliferation is dramatically reduced between passage 6-7, compared to the gradual proliferative decline

observed in Fbx4$^{+/+}$ MEFs (Fig. 4A). Both wild type and null MEFs exhibit similar patterns of senescence-associated p19^{Arf} and p16^{Ink4a} induction (Fig. 4B), suggesting that reduced proliferation is not a result of premature senescence. Furthermore, knockdown of p19^{Arf} bypasses cellular senescence, allowing immortalization of Fbx4$^{+/+}$ and Fbx4$^{-/-}$ MEFs; such immortalized cells do not exhibit proliferative defects (Fig. 4C). Given the reduced proliferation observed in passage 6-7 Fbx4$^{-/-}$ MEFs, it is important to note that these cells are not actively undergoing apoptosis, as caspase 3 cleavage is minimal in both Fbx4$^{+/+}$ and Fbx4$^{-/-}$ MEFs (Fig. 4D). Significantly, Fbx4$^{-/-}$ MEFs accumulate p53 and p21^{Cip1}, as well as γH2AX, consistent with induction of the DNA damage checkpoint in later passages (Fig. 4E). Fbx4$^{-/-}$ cells also accumulate DSB-associated nuclear foci (Fig. 4F), further supporting this notion. Previous studies established that primary MEF proliferation under atmospheric oxygen is limited by oxidative DNA damage, despite maintenance of long telomeres (40). Importantly, while Fbx4$^{-/-}$ MEFs display markers of DNA damage earlier than Fbx4$^{+/+}$ counterparts, the DNA damage in Fbx4$^{-/-}$ MEFs cannot be rescued by culture under physiological oxygen (3% O_2; Fig. 4F). Next, we assessed whether immortalized Fbx4$^{+/+}$ and Fbx4$^{-/-}$ cells are sensitive to S-phase DNA damage. Fbx4$^{+/+}$ and Fbx4$^{-/-}$ cells were synchronized in S-phase, pulsed with 2mM HU for 2 hours, followed by HU washout and treatment with colcemid to arrest cells in metaphase. Metaphase spreads prepared from Fbx4$^{-/-}$ cells exhibited a significant increase in chromosome alterations compared to wild type controls (Fig. 4G). Collectively, these data reveal that loss of Fbx4 triggers nuclear cyclin D1 accumulation, DNA damage checkpoint activation, and ultimately genomic instability.

Previous work established that nuclear cyclin D1 promotes DNA re-replication during S-phase and continued DNA replication in the presence of S-phase DNA damage, thereby facilitating genomic instability; these phenotypes are driven by nuclear cyclin D1/CDK4-mediated *CUL4* repression and Cdt1 stabilization (1, 41). Consistent with these findings, Cdt1 protein is stabilized

throughout S-phase in Fbx4$^{-/-}$ cells, with a concomitant reduction in Cul4A expression (Fig. 5A). Our data revealed attenuated cyclin D1 turnover in primary S-phase Fbx4$^{-/-}$ MEFs (Fig. 3A); furthermore, cyclin D1 degradation in response to S-phase DNA damage is impaired in Fbx4$^{-/-}$ MEFs (Fig. 5B), suggesting that Fbx4 mediates cyclin D1 destruction during unperturbed S-phase progression and following S-phase DNA damage. Since GSK3β phosphorylates Fbx4, triggering ligase dimerization and activation (5), and GSK3β activity increases following S-phase DNA damage (30, 41), we next ascertained whether Fbx4 phosphorylation and ligase activity are regulated by S-phase DNA damage. Treatment of S-phase cells with ionizing radiation enhanced Fbx4 phosphorylation, concomitant with elevated cyclin D1 phosphorylation (Fig. 5C). Moreover, SCF^{Fbx4} E3 ubiquitin ligase activity toward cyclin D1 substrate *in vitro* is markedly increased when SCF^{Fbx4} complexes are purified from S-phase NIH 3T3 cells subjected to ionizing radiation (Fig. 5D). Together, these data indicate that both phosphorylation-dependent cyclin D1 nuclear export, as well as phosphorylation-dependent Fbx4 ligase activation synergize to promote cyclin D1 ubiquitylation following S-phase DNA damage, thereby preserving genome integrity.

Fbx4 loss cooperates with RasV12 *in vitro*

The data provided demonstrate that cyclin D1 is deregulated, leading to its nuclear accumulation in the absence of Fbx4. Because cyclin D1 overexpression cooperates with Ras to induce cellular transformation (34), we considered whether Fbx4$^{+/-}$ or Fbx4$^{-/-}$ primary MEFs were susceptible to transformation induced by expression of only oncogenic Ha-Ras(V12). Infection of early passage MEFs with retroviruses harboring empty vector or oncogenic Ha-Ras(V12) resulted in foci formation in both Fbx4$^{+/-}$ and Fbx4$^{-/-}$ MEFs, but not Fbx4$^{+/+}$ MEFs (Fig. 6A). While overexpression of wild type cyclin D1 alone does not promote cell transformation or tumorigenesis in immune compromised mice (42), expression of cyclin D1 mutants that are stably retained in the

nucleus is oncogenic (3). Critically, Ras-driven transformation in Fbx4$^{-/-}$ primary MEFs is dependent upon cyclin D1/CDK4 activity, as expression of kinase defective CDK4(K35M) or dominant negative cyclin D1T156A suppresses the transforming phenotype (Fig. 6B). Additionally, expression of cyclin D1T156A in spontaneously immortalized cells also suppresses Ras-driven transformation in the absence of Fbx4 (Fig. 6C). To determine whether Fbx4 loss and subsequent nuclear accumulation of endogenous cyclin D1 permits spontaneous cellular transformation, we examined the capacity of multiple immortalized cell lines of each genotype to form foci *in vitro*. While immortalized Fbx4$^{+/+}$ cells were refractory to spontaneous transformation, Fbx4$^{+/-}$, and to a greater extent, Fbx4$^{-/-}$ cells readily exhibited spontaneous transformation (Fig. 6D), suggesting that Fbx4 plays a requisite role in suppressing cellular transformation *in vitro*.

Fbx4$^{+/-}$ and Fbx4$^{-/-}$ mice are tumor prone

Given the observed cyclin D1 accumulation in normal tissues derived from Fbx4$^{+/-}$ and Fbx4$^{-/-}$ mice and neoplastic transformation phenotype *in vitro*, we interrogated whether Fbx4$^{+/-}$ and Fbx4$^{-/-}$ mice develop spontaneous tumors with increasing age. We monitored mice for up to 24 months and observed significant spontaneous tumor formation in both Fbx4$^{+/-}$ and Fbx4$^{-/-}$ mice (Fig. 7A). Fbx4$^{+/-}$ and Fbx4$^{-/-}$ mice exhibit tumors of lymphoblastic lineage, frequent intense myeloid proliferation resulting from severe extramedullary hematopoiesis (EMH), and early myeloid malignancy. These mice develop large cell lymphomas, as confirmed by flow cytometric and immunohistochemical analysis (Table 1). Additionally, dendritic cell tumors/histiocytic sarcomas of the spleen, thymus and intestinal wall/mesentery, liver hemangiomas and hepatocellular carcinoma, and tumors of the mammary and uterine epithelium were observed (Table 1).

Fbx4$^{+/-}$ and Fbx4$^{-/-}$ mice succumb to significant tumor burden with a mean survival of 23 months (Fig. 7A*)*. Importantly, 60.6 percent and 64.3 percent of Fbx4$^{+/-}$ and Fbx4$^{-/-}$ mice,

respectively exhibit significant pathology before 24 months of age, highlighting the robust penetrance of these phenotypes. To examine whether tumorigenesis in $Fbx4^{+/-}$ mice was due to haploinsufficiency or loss of heterozygosity (LOH), Fbx4 protein expression was analyzed in representative tumor samples. Immunoblot analyses revealed that a majority of $Fbx4^{+/-}$ tumors retain Fbx4 expression, albeit with an approximate 50 percent reduction in expression compared to wild type, suggesting that Fbx4 dosage is an important determinant in malignant transformation (Fig. 7B). Consistent with this observation, one wild-type age matched control mouse exhibited severe extramedullary hematopoiesis, a phenotype typically observed in the $Fbx4^{+/-}$ and $Fbx4^{-/-}$ mice; strikingly, immunoblot analysis revealed significant Fbx4 downregulation in this spleen.

Since normal and pre-malignant $Fbx4^{+/-}$ and $Fbx4^{-/-}$ tissues exhibit cyclin D1 protein accumulation, we ascertained whether cyclin D1 protein expression is elevated in the various tumors. Consistently, elevated cyclin D1 protein was apparent in a majority of lymphomas originating in the mesenteric node of both $Fbx4^{+/-}$ and $Fbx4^{-/-}$ mice, and in livers exhibiting lymphoma infiltrates or hepatocellular carcinoma (Fig. 7C, D). Furthermore, intestinal histiocytic sarcomas and mesenteric node lymphomas exhibit nuclear cyclin D1 accumulation, correlating with increased proliferation as evidenced by Ki-67 staining (Fig. 7E). Immunoblot and immunohistochemical analyses also revealed a marked induction of γH2AX and phosphorylated ATM, respectively, in lymphoid tumors, consistent with nuclear cyclin D1-driven genomic instability (Fig. 7E, F). To further assess sensitivity to genomic instability in wild type and $Fbx4^{+/-}$ lymphoma cells, we prepared single cell suspensions of primary lymphocytes or lymphoma cells and assessed chromosome alterations following an HU pulse; loss of Fbx4 significantly increases the incidence of chromatid breaks in lymphoma cells compared to normal lymphoid tissue (Fig. 7G). Finally, DNA sequencing of the p53 DNA binding domain in lymphoid tumors revealed a premature stop codon insertion and three distinct deletion mutations in the six tumors analyzed

(data not shown), suggesting that p53 inactivation may contribute to sustained growth in the presence of DNA damage, thereby facilitating neoplastic transformation. Collectively, these data support a requisite role for Fbx4 in maintaining cell homeostasis *in vitro* and *in vivo* by regulating cyclin D1 accumulation.

DISCUSSION

The SCF^{Fbx4} E3 ubiquitin ligase has been implicated in regulating cyclin D1 turnover in cell culture models; further work revealed a significant role for Fbx4 function in maintaining genomic integrity, highlighted by the relative frequency of mutations that impair its biochemical activity in human tumors. Such mutations occur in a hemizygous manner, consistent with the notion that reduced Fbx4 expression is sufficient for cyclin D1 deregulation and neoplastic transformation (5). While this evidence suggests that Fbx4 may function as a tumor suppressor, experiments that directly address this question have not been performed. Our analysis demonstrates that Fbx4 loss promotes cyclin D1 overexpression and tumorigenesis, as a significant increase in age-associated malignancy was observed in $Fbx4^{+/-}$ and $Fbx4^{-/-}$ mice compared to wild type controls. Furthermore, Fbx4 loss in MEFs triggered cyclin D1 stabilization and nuclear localization, and aberrant cyclin D1 regulation in the absence of Fbx4 drives accumulation of DNA damage and subsequent genomic instability, a hallmark of neoplastic transformation. Consistently, loss of Fbx4 facilitates cell transformation *in vitro*, further emphasizing the tumor suppressive properties of Fbx4.

Fbx4 is a tumor suppressor

Both $Fbx4^{+/-}$ and $Fbx4^{-/-}$ aged mice commonly develop lymphoid malignancies involving the mesenteric lymph node, spleen, liver, and intestine, as well as histiocytic sarcomas/dendritic cell tumors of the spleen, thymus and intestine, early myeloid malignancies, as well as mammary, hepatocellular, and uterine carcinomas occurring at lesser frequencies. $Fbx4^{+/-}$ tumors retain Fbx4 expression, consistent with human cancer data revealing hemizygous Fbx4 mutations (5). In addition, $Fbx4^{+/-}$ and $Fbx4^{-/-}$ MEFs are susceptible to single step, Ras-mediated transformation, supporting the notion that Fbx4 functions as a haploinsufficient tumor suppressor. Importantly, this haploinsufficient function of Fbx4 is not unanticipated, as previous work utilizing RNAi revealed

that reduced Fbx4 expression by 60-70 percent is sufficient to promote cyclin D1 stabilization in various epithelial and fibroblast cell lines and anchorage-independent growth *in vitro* (5). While an elevation in cyclin D1 protein in $Fbx4^{+/-}$ and $Fbx4^{-/-}$ in epithelial tissue might be anticipated, the increased cyclin D1 expression in lymphocytes, which typically do not express cyclin D1, and lymphoid tumors were indeed enlightening. These results support a requisite role for post-translational degradation as a means to limit cyclin D1 accumulation in normal lymphoid tissue, thereby highlighting the tumor suppressive function of Fbx4 in this tissue. Interestingly, not all tissues exhibiting elevated cyclin D1 develop neoplastic lesions; for example cyclin D1 is elevated in normal $Fbx4^{+/-}$ and $Fbx4^{-/-}$ lung tissue; however, spontaneous lung adenocarcinomas were not observed. This raises the possibility that the absence of Fbx4 can trigger compensatory pathways for cyclin D1/CDK4 regulation, ultimately antagonizing nuclear function when Fbx4-mediated degradation is impaired.

$Fbx4^{+/-}$ and $Fbx4^{-/-}$ mice develop tumors with a protracted latency that is comparable to pituitary tumors observed in $p18^{Ink4c-/-}$ mice, sarcomas in $p15^{Ink4b-/-}$ mice, and B-cell lymphomas, lung adenocarcinomas, and hepatocellular carcinomas in $U19/EAF2^{-/-}$ mice (29, 53). Although tumors arise in aged mice, it is important to note that this is a remarkably penetrant phenotype, with 38 percent of $Fbx4^{+/-}$ and $Fbx4^{-/-}$ mice exhibiting substantial lymphoma burden and 23.4 percent exhibiting EMH before 24 months of age. Furthermore, the frequent incidence of EMH and associated early myeloid malignancy suggests bone marrow failure, and it is of interest to assess the role of Fbx4 in hematopoietic development and bone marrow function in future work.

Loss of Fbx4 promotes cyclin D1 nuclear accumulation and DNA damage

Previous work has linked nuclear cyclin D1 accumulation with tumorigenesis (3, 15, 33). However, the rare incidence of mutations in cyclin D1 that impair its nuclear export and

cytoplasmic degradation suggests that other components of the cyclin D1 regulatory machinery, such as Fbx4, are the major targets that confer tumor susceptibility in vivo. Consistent with this notion, we observed a substantial extension of cyclin D1 half-life in S-phase Fbx4$^{-/-}$ MEFs, with a significant increase in the rate of proliferation. Importantly, accumulating evidence suggests that cyclin D1 nuclear accumulation during S-phase, rather than overt overexpression, underlies its oncogenic function (1, 2, 15, 33).

Consistent with the aforementioned nuclear cyclin D1 phenotype, the initial proliferative advantage observed in Fbx4$^{-/-}$ MEFs dramatically decreases in later passages, suggesting that cells either activate a senescence program prematurely or decrease proliferation as a consequence of DNA damage and/or additional stress responses. Our data support the generation of DNA damage, as DNA damage checkpoint activation is clearly evident in passage 3-5 MEFs. Importantly, DNA damage observed in Fbx4$^{-/-}$ MEFs is not simply due to oxidative stress, as growth under physiological (3%) O_2 tension does not reduce DNA damage. In addition, DNA damage is not likely to result from stabilization of the other known Fbx4 substrate, Trf1, given that telomere uncapping effects of Trf1 stabilization would take many generations, due to the extremely long telomeres observed in most laboratory mouse lines (31). Nuclear cyclin D1 retention during S-phase promotes DNA re-replication and subsequent DNA damage checkpoint activation; mechanistically, nuclear cyclin D1/CDK4 kinase activity is necessary for elevated histone arginine methylation at the *Cul4* promoters, *Cul4* repression, and consequent stabilization of the replication factor Cdt1 (1, 2). In fact, tumors arising in Fbx4$^{+/-}$ and Fbx4$^{-/-}$ mice exhibit a dramatic increase in histone 4 arginine 3 symmetric di-methylation, and Fbx4$^{-/-}$ MEFs exhibit Cdt1 stabilization in S-phase, with a concomitant reduction in Cul4 levels, supporting the notion that Cdt1 stabilization downstream of nuclear cyclin D1/CDK4 activity drives DNA damage accumulation.

Our previous and current data reveal a tightly regulated mechanistic program for cyclin D1 control in S-phase and following DNA damage. Fbx4 serine 12 phosphorylation, an event preceding ligase dimerization and activation, ensures an increased rate of cyclin D1 ubiquitylation following the G1/S transition. Intriguingly, both nuclear cyclin D1 threonine 286 and cytoplasmic Fbx4 serine 12 are phosphorylated by GSK3β at this point, highlighting the dual regulatory role post-translational modifications play in coordinating timely cyclin D1 destruction (5, 13). Therefore, it is not surprising that both cyclin D1 threonine 286 and Fbx4 serine 12 phosphorylation events are induced above basal levels following DNA damage, thereby facilitating increased ubiquitin ligase activity toward cyclin D1. Considering that nuclear cyclin D1 promotes DNA re-replication and checkpoint activation (1), and that impaired cyclin D1 degradation in response to S-phase DNA damage drives genomic instability (41), loss or functional inactivation of Fbx4 provides oncogenic insults necessary for neoplastic transformation.

Collectively, our current work supports a model where Fbx4 expression is essential for cell homeostasis in somatic cells. Fbx4 ablation predisposes mice to multiple tumor phenotypes, with concomitant cyclin D1 deregulation and nuclear accumulation. Furthermore, our data suggest that Fbx4 status is an important determinant of neoplastic potential in cells harboring wild type cyclin D1 overexpression, functioning as a haploinsufficient tumor suppressor. Identification of novel Fbx4 substrates will elucidate additional signaling pathways contributing to the neoplastic phenotype in $Fbx4^{-/-}$ animals, functioning in concert with cyclin D1, and future development of Fbx4 conditionally-deficient mice will enable Fbx4 ablation in various adult tissues, mirroring the somatic inactivating mutations observed in human cancers.

ACKNOWLEDGEMENTS

The authors thank Petia Zamfirova, Margarita Romero, and Jesi Kim for technical assistance, Dr. Serge Fuchs for critical reading of the manuscript, the AFCRI histology core for assistance with paraffin embedding and sectioning, Drs. Oren Gilad and Eric Brown for providing $p19^{Arf}$ shRNA lentivirus, and the NIH P30 Center for Molecular Studies in Digestive and Liver Diseases and its Morphology and Molecular Biology Cores. This work was supported by grants from the National Institutes of Health (CA133154), a Leukemia and Lymphoma Scholar Award (JAD) and P01-CA098101 (AKR and JAD).

FIGURE LEGENDS

Figure 1. Generation of $Fbx4^{+/-}$ and $Fbx4^{-/-}$ mice. (A) Targeted disruption of the mouse *Fbx4* locus. Exon 2, encoding the F-box, is flanked by LoxP sites with a downstream neomycin (NEO) resistance cassette flanked by a third LoxP site. (B) Southern blot of a targeted ES clone (denoted by *) using 5' probe shown in A. (C) Genotyping of $Fbx4^{+/+}$, $Fbx4^{+/-}$, and $Fbx4^{-/-}$ d14 embryos from a heterozygous cross using tail DNA and PCR primers denoted in (A).

Figure 2. Cyclin D1 accumulation in $Fbx4^{+/-}$ and $Fbx4^{-/-}$ tissues and MEFs. Tissues were harvested from 1-2 month old mice of each genotype, and lysates prepared for SDS-PAGE and immunoblotted as indicated. Cyclin D1 accumulation was assessed in mammary glands (A), lungs (B), thymus (C), spleen (D), and primary MEFs (E). (F) Cyclin D1 message is equivalent in $Fbx4^{+/+}$, $Fbx4^{+/-}$, and $Fbx4^{-/-}$ MEFs. RT-PCR was performed on total RNA isolated from MEFs of the indicated genotype using PCR primers specific for cyclin D1 and the housekeeping gene HPRT as a control.

Figure 3. Fbx4 loss promotes cyclin D1 stabilization and nuclear accumulation in MEFs. (A) Cyclin D1 $t_{1/2}$ is extended in S-phase $Fbx4^{-/-}$ MEFs. Top panel: synchronous S-phase MEFs were treated with cycloheximide (CHX) as indicated; cell lysates were subjected to SDS-PAGE and immunoblotted for cyclin D1, Fbx4, and cyclin A as an S-phase marker. Bottom panel: calculated cyclin D1 $t_{1/2}$ for two independent replicates per genotype. (B) Nuclear cyclin D1 accumulation in $Fbx4^{-/-}$ MEFs. Top panel: passage 3 MEFs were stained with cyclin D1-specific antibodies and DAPI. Images were captured at 20x magnification, with equal exposure. Bottom panel: quantification of nuclear cyclin D1 staining. (C) $Fbx4^{-/-}$ MEFs exhibit increased proliferation. $1x10^5$ $Fbx4^{+/+}$ and $Fbx4^{-/-}$ MEFs (passage 2) were plated in duplicate on 35mm plates and counted daily.

(D) Elevated cyclin D1 protein in S-phase Fbx4$^{-/-}$ cells. p19shRNA-immortalized cells were synchronized by serum starvation, and lysates were immunoblotted as indicated. (E) Phosphorylated cyclin D1 accumulates in S-phase Fbx4$^{-/-}$ cells. Total cyclin D1 was immunoprecipitated from S-phase cell lysates and immunoblotted for phospho-T286 cyclin D1 (pT286 D1) and total cyclin D1. (F) Cyclin D1 ubiquitylation following the G1/S transition is impaired in Fbx4$^{-/-}$ cells. Cells were synchronized by serum starvation and stimulated to enter early S-phase. Total cyclin D1 was immuno-precipitated from cell lysates, subjected to SDS-PAGE, and immunoblotted to visualize cyclin D1 laddering. Top panel: pT286 cyclin D1 immunoblot. Middle panel: total ubiquitin immunoblot. Bottom panel: total cyclin D1 immunoblot.

Figure 4. Enhanced proliferation is antagonized by DNA damage in Fbx4$^{+/-}$ and Fbx4$^{-/-}$ MEFs. (A) MEFs were cultured on a 3T9 passage protocol ($9x10^5$ cells passaged every three days, at least two biological replicates/genotype). Absolute cell count at each passage is displayed. (B) Expression of senescence-associated p19^{Arf} and p16^{Ink4a} in primary MEFs. (C) Knockdown of p19^{Arf} rescues cellular senescence, promoting immortalization. Black curves represent passages of uninfected MEFs; gray curves represent MEFs infected with p19^{Arf} shRNA at passage 4. Immortalized cells proliferate indefinitely beyond passage 8. (D) Minimal caspase 3 cleavage in Fbx4$^{+/+}$ and Fbx4$^{-/-}$ MEFs. Passage 5 MEFs (3 independent biological replicates per genotype) were harvested, followed by western analysis for total and cleaved caspase 3 as a marker for induction of apoptosis. (E) Enhanced p53 and γH2AX induction in Fbx4$^{-/-}$ MEFs. Passage 5 MEF lysates were prepared from two independent isolates/genotype and immunoblotted as indicated. (F) Fbx4$^{-/-}$ MEFs accumulate DNA damage foci. Top panel: Passage 3 MEFs were cultured on coverslips under normoxia (21% O_2) or physiological oxygen tension (3% O_2). Cells were fixed, stained with γH2AX-specific antibodies, and visualized by immunofluorescence. Images were taken at 60x

magnification with equal exposure time. Bottom panel: quantification of the percentage of cells exhibiting DNA damage foci. (G) Increased incidence of chromosome alterations in Fbx4$^{-/-}$ MEFs challenged with hydroxyurea (HU). Two independent immortalized MEF lines per genotype were synchronized by serum starvation, and cells in mid-S-phase were treated with 2mM HU for 2 hours, followed by HU washout and colcemid treatment for 2 hours for metaphase arrest. Metaphase spreads were prepared and stained with Giemsa to visualize chromosome alterations. Left panel: representative images of chromatid breaks. Right panel: quantification of the average number of chromatid breaks per cell.

Figure 5. DNA damage regulates cyclin D1 stability and Fbx4 ligase activation. (A) Stabilization of Cdt1 in immortalized, S-phase-synchronized Fbx4$^{-/-}$ cells. Cells synchronized by serum starvation were serum stimulated for the indicated time (12h=late G1; 14, 16, 18h=G1/S, mid-S, and late S-phase, respectively), harvested, and subjected to SDS-PAGE and immunoblot analysis for the indicated proteins. (B) S-phase DNA damage-mediated cyclin D1 degradation is attenuated in Fbx4$^{-/-}$ MEFs. Immortalized cells were synchronized by serum starvation followed by treatment with 2mM HU; cell lysates were immunoblotted as indicated. (C) Enhanced Fbx4 phosphorylation following S-phase DNA damage. Asynchronous NIH 3T3 cells, or cells synchronized by serum starvation and stimulated (12h=G1, 16h=S-phase) were irradiated, followed by recovery for 30 minutes. Cells were harvested and lysates were immunoprecipitated with phospho-serine 12 (pS12 Fbx4) specific antibodies (top panel) to visualize induction of phosphorylation. Total input lysate immunoblots are shown below. (D) SCF^{Fbx4} ligase activity toward cyclin D1 substrate is enhanced following S-phase DNA damage. SCF^{Fbx4} complexes were immunoprecipitated from S-phase NIH 3T3 cells with or without induction of DNA damage using Fbx4-specific antibodies. Fbx4-containing complexes served as a ligase source for *in vitro*

ubiquitylation reactions with Sf9-purified cyclin D1/CDK4 as substrate, in the presence of E1, E2, ubiquitin, and ATP.

Figure 6. Fbx4 loss drives cell transformation *in vitro*. (A) Loss of Fbx4 synergizes with oncogenic Ha-RasV12 to promote cell transformation. Primary MEFs (passage 3) were infected with retroviruses harboring empty vector (EV) or Ha-RasV12 (Ras) constructs. $1.5x10^5$ cells were plated in duplicate on 35mm plates, grown for 21 days to allow foci formation, and stained with Giemsa to visualize foci. Bottom panel: quantification of foci number for duplicate plates of each genotype. (B) Primary passage 4 MEFs were transfected with the indicated constructs and plated in duplicate as in (A) to assess foci formation in the presence of kinase-deficient CDK4 K35M and dominant negative cyclin D1T156A. Bottom panel: quantification of foci number for duplicate plates. (C) Expression of cyclin D1T156A suppresses Ha-RasV12-mediated transformation. Low passage spontaneously immortalized cells were transfected with the indicated constructs. 48 hours post-transfection, cells were trypsinized and plated in duplicate to assess foci formation as in (A). (D) Spontaneous transformation in immortalized cells. p19shRNA-immortalized cells of each genotype (two independent biological replicate cell lines, passage 15) were plated at a density of $1.5x10^5$ cells on 35mm plates in triplicate and grown as in (A).

Figure 7. $Fbx4^{+/-}$ and $Fbx4^{-/-}$ mice are tumor prone. (A) Kaplan-Meier curves showing percentage tumor-free survival of $Fbx4^{+/+}$, $Fbx4^{+/-}$, and $Fbx4^{-/-}$ mice to 24 months. (B) Fbx4 haploinsufficiency. Representative tumors arising in $Fbx4^{+/-}$ mice were assessed for Fbx4 protein expression by western blot; only one of four tumors analyzed downregulated Fbx4 expression. (C) $Fbx4^{+/-}$ and $Fbx4^{-/-}$ lymphomas exhibit cyclin D1 accumulation. Lysates prepared from wild type age matched spleens, $Fbx4^{-/-}$ spleens, and mesenteric node lymphomas were subjected to SDS-PAGE and immunoblotting

as indicated. (D) Fbx4$^{+/-}$ liver tumors exhibit cyclin D1 accumulation. Lysates prepared from Fbx4$^{+/-}$ livers harboring lymphoma, hepatocellular carcinoma (HCC) or hemangioma and normal age-matched livers were analyzed by immunoblot analysis for cyclin D1 levels. (E) Representative H&E and immunohistochemical (IHC) staining for cyclin D1 and Ki-67 as a marker of proliferation in normal intestinal epithelium, Fbx4$^{+/-}$ histiocytic sarcoma of the intestinal muscle wall, and Fbx4$^{-/-}$ primary lymphoma of the mesenteric node. (F) IHC staining for DNA damage markers phosphorylated ATM and γH2AX in Fbx4$^{-/-}$ lymphoma or age-matched wild type lymphoid tissue. (G) Increased incidence of chromosome alterations in Fbx4$^{-/-}$ lymphoma cells. Mesenteric Node and splenic lymphoma cells or wild type lymphocytes were pulsed with 2mM HU for 2 hours, followed by HU washout and colcemid treatment for 2 hours for metaphase arrest. Metaphase spreads were prepared and stained with Giemsa to visualize chromosome alterations. Top panel: representative images of chromatid breaks. Bottom panel: quantification of the average number of chromatid breaks per cell.

Table 1. Summary of pathology observed in Fbx4$^{+/-}$ and Fbx4$^{-/-}$ mice. Fbx4$^{+/-}$ and Fbx4$^{-/-}$ mice included as events in the Kaplan-Meier survival analysis frequently develop large cell lymphoblastic lymphomas involving the mesenteric lymph node, spleen, thymus, Peyer's patches of the intestine, and liver. A large percentage of mice also exhibit extramedullary hematopoiesis (EMH) and intense myeloid proliferation in the spleen and less frequently, liver. This is also associated with early myeloid tumor formation. Less commonly observed malignancies include dendritic cell/histiocytic sarcomas, hemangioma, uterine tumor, and mammary carcinoma. Analysis of several mice independent of the Kaplan-Meier cohort also revealed an additional case of intestinal histiocytic sarcoma and a case of hepatocellular carcinoma.

REFERENCES

1. **Aggarwal, P., M. D. Lessie, D. I. Lin, L. Pontano, A. B. Gladden, B. Nuskey, A. Goradia, M. A. Wasik, A. J. Klein-Szanto, A. K. Rustgi, C. H. Bassing, and J. A. Diehl.** 2007. Nuclear accumulation of cyclin D1 during S phase inhibits Cul4-dependent Cdt1 proteolysis and triggers p53-dependent DNA rereplication. Genes Dev **21:**2908-22.

2. **Aggarwal, P., L. P. Vaites, J. K. Kim, H. Mellert, B. Gurung, H. Nakagawa, M. Herlyn, X. Hua, A. K. Rustgi, S. B. McMahon, and J. A. Diehl.** Nuclear cyclin D1/CDK4 kinase regulates CUL4 expression and triggers neoplastic growth via activation of the PRMT5 methyltransferase. Cancer Cell **18:**329-40.

3. **Alt, J. R., J. L. Cleveland, M. Hannink, and J. A. Diehl.** 2000. Phosphorylation-dependent regulation of cyclin D1 nuclear export and cyclin D1-dependent cellular transformation. Genes Dev **14:**3102-14.

4. **Bani-Hani, K., I. G. Martin, L. J. Hardie, N. Mapstone, J. A. Briggs, D. Forman, and C. P. Wild.** 2000. Prospective study of cyclin D1 overexpression in Barrett's esophagus: association with increased risk of adenocarcinoma. J Natl Cancer Inst **92:**1316-21.

5. **Barbash, O., P. Zamfirova, D. I. Lin, X. Chen, K. Yang, H. Nakagawa, F. Lu, A. K. Rustgi, and J. A. Diehl.** 2008. Mutations in Fbx4 Inhibit Dimerization of the SCF(Fbx4) Ligase and Contribute to Cyclin D1 Overexpression in Human Cancer. Cancer Cell **14:**68-78.

6. **Bartkova, J., J. Lukas, H. Muller, D. Lutzhoft, M. Strauss, and J. Bartek.** 1994. Cyclin D1 protein expression and function in human breast cancer. Int J Cancer **57:**353-61.

7. **Bartkova, J., J. Lukas, H. Muller, M. Strauss, B. Gusterson, and J. Bartek.** 1995. Abnormal patterns of D-type cyclin expression and G1 regulation in human head and neck cancer. Cancer Res **55:**949-56.

8. **Bartkova, J., J. Lukas, M. Strauss, and J. Bartek.** 1994. The PRAD-1/cyclin D1 oncogene product accumulates aberrantly in a subset of colorectal carcinomas. Int J Cancer **58:**568-73.

9. **Benzeno, S., F. Lu, M. Guo, O. Barbash, F. Zhang, J. G. Herman, P. S. Klein, A. Rustgi, and J. A. Diehl.** 2006. Identification of mutations that disrupt phosphorylation-dependent nuclear export of cyclin D1. Oncogene **25:**6291-303.

10. **Busino, L., M. Donzelli, M. Chiesa, D. Guardavaccaro, D. Ganoth, N. V. Dorrello, A. Hershko, M. Pagano, and G. F. Draetta.** 2003. Degradation of Cdc25A by beta-TrCP during S phase and in response to DNA damage. Nature **426:**87-91.

11. **Carrano, A. C., E. Eytan, A. Hershko, and M. Pagano.** 1999. SKP2 is required for ubiquitin-mediated degradation of the CDK inhibitor p27. Nat Cell Biol **1:**193-9.

12. **Deshaies, R. J.** 1999. SCF and Cullin/Ring H2-based ubiquitin ligases. Annu Rev Cell Dev Biol **15:**435-67.

13. **Diehl, J. A., M. Cheng, M. F. Roussel, and C. J. Sherr.** 1998. Glycogen synthase kinase-3beta regulates cyclin D1 proteolysis and subcellular localization. Genes Dev **12:**3499-511.

14. **Gillett, C., V. Fantl, R. Smith, C. Fisher, J. Bartek, C. Dickson, D. Barnes, and G. Peters.** 1994. Amplification and overexpression of cyclin D1 in breast cancer detected by immunohistochemical staining. Cancer Res **54:**1812-7.

15. **Gladden AB, W. R., Aggarwal P, Wasik MA, Diehl JA** 2006. Expression of constitutively nuclear cyclin D1 in murine lymphocytes induces B-cell lymphoma Oncogene **25:**998-1007.

16. **Guardavaccaro, D., Y. Kudo, J. Boulaire, M. Barchi, L. Busino, M. Donzelli, F. Margottin-Goguet, P. K. Jackson, L. Yamasaki, and M. Pagano.** 2003. Control of meiotic and mitotic progression by the F box protein beta-Trcp1 in vivo. Dev Cell **4:**799-812.

17. **Hao, B., S. Oehlmann, M. E. Sowa, J. W. Harper, and N. P. Pavletich.** 2007. Structure of a Fbw7-Skp1-cyclin E complex: multisite-phosphorylated substrate recognition by SCF ubiquitin ligases. Mol Cell **26:**131-43.

18. **Hatakeyama, S., M. Kitagawa, K. Nakayama, M. Shirane, M. Matsumoto, K. Hattori, H. Higashi, H. Nakano, K. Okumura, K. Onoe, and R. A. Good.** 1999. Ubiquitin-dependent degradation of IkappaBalpha is mediated by a ubiquitin ligase Skp1/Cul 1/F-box protein FWD1. Proc Natl Acad Sci U S A **96:**3859-63.

19. **Herman, J. G., A. Merlo, L. Mao, R. G. Lapidus, J. P. Issa, N. E. Davidson, D. Sidransky, and S. B. Baylin.** 1995. Inactivation of the CDKN2/p16/MTS1 gene is frequently associated with aberrant DNA methylation in all common human cancers. Cancer Res **55:**4525-30.

20. **Hershko, A., and A. Ciechanover.** 1998. The ubiquitin system. Annu Rev Biochem **67:**425-79.

21. **Hibberts, N. A., D. J. Simpson, J. E. Bicknell, J. C. Broome, P. R. Hoban, R. N. Clayton, and W. E. Farrell.** 1999. Analysis of cyclin D1 (CCND1) allelic imbalance and overexpression in sporadic human pituitary tumors. Clin Cancer Res **5:**2133-9.

22. **Hosokawa, Y., and A. Arnold.** 1998. Mechanism of cyclin D1 (CCND1, PRAD1) overexpression in human cancer cells: analysis of allele-specific expression. Genes Chromosomes Cancer **22:**66-71.

23. **Hosokawa, Y., T. Joh, Y. Maeda, A. Arnold, and M. Seto.** 1999. Cyclin D1/PRAD1/BCL-1 alternative transcript [B] protein product in B-lymphoid malignancies with t(11;14)(q13;q32) translocation. Int J Cancer **81:**616-9.

24. **Jin, J., T. Shirogane, L. Xu, G. Nalepa, J. Qin, S. J. Elledge, and J. W. Harper.** 2003. SCFbeta-TRCP links Chk1 signaling to degradation of the Cdc25A protein phosphatase. Genes Dev **17:**3062-74.

25. **Jin, M., S. Inoue, T. Umemura, J. Moriya, M. Arakawa, K. Nagashima, and H. Kato.** 2001. Cyclin D1, p16 and retinoblastoma gene product expression as a predictor for prognosis in non-small cell lung cancer at stages I and II. Lung Cancer **34:**207-18.

26. **Kitagawa, M., S. Hatakeyama, M. Shirane, M. Matsumoto, N. Ishida, K. Hattori, I. Nakamichi, A. Kikuchi, and K. Nakayama.** 1999. An F-box protein, FWD1, mediates ubiquitin-dependent proteolysis of beta-catenin. EMBO J **18:**2401-10.

27. **Koepp, D. M., L. K. Schaefer, X. Ye, K. Keyomarsi, C. Chu, J. W. Harper, and S. J. Elledge.** 2001. Phosphorylation-dependent ubiquitination of cyclin E by the SCFFbw7 ubiquitin ligase. Science **294:**173-7.

28. **Latres, E., D. S. Chiaur, and M. Pagano.** 1999. The human F box protein beta-Trcp associates with the Cul1/Skp1 complex and regulates the stability of beta-catenin. Oncogene **18:**849-54.

29. **Latres, E., M. Malumbres, R. Sotillo, J. Martin, S. Ortega, J. Martin-Caballero, J. M. Flores, C. Cordon-Cardo, and M. Barbacid.** 2000. Limited overlapping roles of P15(INK4b) and P18(INK4c) cell cycle inhibitors in proliferation and tumorigenesis. EMBO J **19:**3496-506.

30. **Lee, J. Y., S. J. Yu, Y. G. Park, J. Kim, and J. Sohn.** 2007. Glycogen synthase kinase 3beta phosphorylates p21WAF1/CIP1 for proteasomal degradation after UV irradiation. Mol Cell Biol **27:**3187-98.

31. **Lee, T. H., K. Perrem, J. W. Harper, K. P. Lu, and X. Z. Zhou.** 2006. The F-box protein FBX4 targets PIN2/TRF1 for ubiquitin-mediated degradation and regulates telomere maintenance. J Biol Chem **281:**759-68.

32. **Lin, D. I., O. Barbash, K. G. Kumar, J. D. Weber, J. W. Harper, A. J. Klein-Szanto, A. Rustgi, S. Y. Fuchs, and J. A. Diehl.** 2006. Phosphorylation-dependent ubiquitination of cyclin D1 by the SCF(FBX4-alphaB crystallin) complex. Mol Cell **24:**355-66.

33. **Lin, D. I., M. D. Lessie, A. B. Gladden, C. H. Bassing, K. U. Wagner, and J. A. Diehl.** 2007. Disruption of cyclin D1 nuclear export and proteolysis accelerates mammary carcinogenesis. Oncogene.

34. **Lovec, H., A. Sewing, F. C. Lucibello, R. Muller, and T. Moroy.** 1994. Oncogenic activity of cyclin D1 revealed through cooperation with Ha-ras: link between cell cycle control and malignant transformation. Oncogene **9:**323-6.

35. **Lu, F., A. B. Gladden, and J. A. Diehl.** 2003. An alternatively spliced cyclin D1 isoform, cyclin D1b, is a nuclear oncogene. Cancer Res **63:**7056-61.

36. **Margottin-Goguet, F., J. Y. Hsu, A. Loktev, H. M. Hsieh, J. D. Reimann, and P. K. Jackson.** 2003. Prophase destruction of Emi1 by the SCF(betaTrCP/Slimb) ubiquitin ligase activates the anaphase promoting complex to allow progression beyond prometaphase. Dev Cell **4:**813-26.

37. **Moreno-Bueno, G., S. Rodriguez-Perales, C. Sanchez-Estevez, D. Hardisson, D. Sarrio, J. Prat, J. C. Cigudosa, X. Matias-Guiu, and J. Palacios.** 2003. Cyclin D1 gene (CCND1) mutations in endometrial cancer. Oncogene **22:**6115-8.

38. **Nakayama, K., S. Hatakeyama, S. Maruyama, A. Kikuchi, K. Onoe, R. A. Good, and K. I. Nakayama.** 2003. Impaired degradation of inhibitory subunit of NF-kappa B (I kappa B) and beta-catenin as a result of targeted disruption of the beta-TrCP1 gene. Proc Natl Acad Sci U S A **100:**8752-7.

39. **Nakayama, K. I., and K. Nakayama.** 2005. Regulation of the cell cycle by SCF-type ubiquitin ligases. Semin Cell Dev Biol **16:**323-33.

40. **Parrinello, S., E. Samper, A. Krtolica, J. Goldstein, S. Melov, and J. Campisi.** 2003. Oxygen sensitivity severely limits the replicative lifespan of murine fibroblasts. Nat Cell Biol **5:**741-7.

41. **Pontano, L. L., P. Aggarwal, O. Barbash, E. J. Brown, C. H. Bassing, and J. A. Diehl.** 2008. Genotoxic stress-induced cyclin D1 phosphorylation and proteolysis are required for genomic stability. Mol Cell Biol **28:**7245-58.

42. **Quelle, D. E., R. A. Ashmun, S. A. Shurtleff, J. Y. Kato, D. Bar-Sagi, M. F. Roussel, and C. J. Sherr.** 1993. Overexpression of mouse D-type cyclins accelerates G1 phase in rodent fibroblasts. Genes Dev **7:**1559-71.

43. **Skowyra, D., K. L. Craig, M. Tyers, S. J. Elledge, and J. W. Harper.** 1997. F-box proteins are receptors that recruit phosphorylated substrates to the SCF ubiquitin-ligase complex. Cell **91:**209-19.

44. **Suzuki, H., T. Chiba, T. Suzuki, T. Fujita, T. Ikenoue, M. Omata, K. Furuichi, H. Shikama, and K. Tanaka.** 2000. Homodimer of two F-box proteins betaTrCP1 or betaTrCP2 binds to IkappaBalpha for signal-dependent ubiquitination. J Biol Chem **275:**2877-84.

45. **Tan, P., S. Y. Fuchs, A. Chen, K. Wu, C. Gomez, Z. Ronai, and Z. Q. Pan.** 1999. Recruitment of a ROC1-CUL1 ubiquitin ligase by Skp1 and HOS to catalyze the ubiquitination of I kappa B alpha. Mol Cell **3:**527-33.

46. **Tang, X., S. Orlicky, Z. Lin, A. Willems, D. Neculai, D. Ceccarelli, F. Mercurio, B. H. Shilton, F. Sicheri, and M. Tyers.** 2007. Suprafacial orientation of the SCFCdc4 dimer accommodates multiple geometries for substrate ubiquitination. Cell **129:**1165-76.

47. **Tetzlaff, M. T., W. Yu, M. Li, P. Zhang, M. Finegold, K. Mahon, J. W. Harper, R. J. Schwartz, and S. J. Elledge.** 2004. Defective cardiovascular development and elevated cyclin E and Notch proteins in mice lacking the Fbw7 F-box protein. Proc Natl Acad Sci U S A **101:**3338-45.

48. **Tsunematsu, R., K. Nakayama, Y. Oike, M. Nishiyama, N. Ishida, S. Hatakeyama, Y. Bessho, R. Kageyama, T. Suda, and K. I. Nakayama.** 2004. Mouse Fbw7/Sel-10/Cdc4 is required for notch degradation during vascular development. J Biol Chem **279:**9417-23.

49. **Welcker, M., A. Orian, J. Jin, J. A. Grim, J. W. Harper, R. N. Eisenman, and B. E. Clurman.** 2004. The Fbw7 tumor suppressor regulates glycogen synthase kinase 3 phosphorylation-dependent c-Myc protein degradation. Proc Natl Acad Sci U S A **101:**9085-90.

50. **Welcker, M., J. Singer, K. R. Loeb, J. Grim, A. Bloecher, M. Gurien-West, B. E. Clurman, and J. M. Roberts.** 2003. Multisite phosphorylation by Cdk2 and GSK3 controls cyclin E degradation. Mol Cell **12:**381-92.

51. **Winston, J. T., D. M. Koepp, C. Zhu, S. J. Elledge, and J. W. Harper.** 1999. A family of mammalian F-box proteins. Curr Biol **9:**1180-2.

52. **Winston, J. T., P. Strack, P. Beer-Romero, C. Y. Chu, S. J. Elledge, and J. W. Harper.** 1999. The SCFbeta-TRCP-ubiquitin ligase complex associates specifically with phosphorylated destruction motifs in IkappaBalpha and beta-catenin and stimulates IkappaBalpha ubiquitination in vitro. Genes Dev **13:**270-83.

53. **Xiao, W., Q. Zhang, G. Habermacher, X. Yang, A. Y. Zhang, X. Cai, J. Hahn, J. Liu, M. Pins, L. Doglio, R. Dhir, J. Gingrich, and Z. Wang.** 2008. U19/Eaf2 knockout causes lung adenocarcinoma, B-cell lymphoma, hepatocellular carcinoma and prostatic intraepithelial neoplasia. Oncogene **27:**1536-44.

54. **Yada, M., S. Hatakeyama, T. Kamura, M. Nishiyama, R. Tsunematsu, H. Imaki, N. Ishida, F. Okumura, K. Nakayama, and K. I. Nakayama.** 2004. Phosphorylation-dependent degradation of c-Myc is mediated by the F-box protein Fbw7. EMBO J **23:**2116-25.

55. **Ye, X., G. Nalepa, M. Welcker, B. M. Kessler, E. Spooner, J. Qin, S. J. Elledge, B. E. Clurman, and J. W. Harper.** 2004. Recognition of phosphodegron motifs in human cyclin E by the SCF(Fbw7) ubiquitin ligase. J Biol Chem **279:**50110-9.

Figure 1

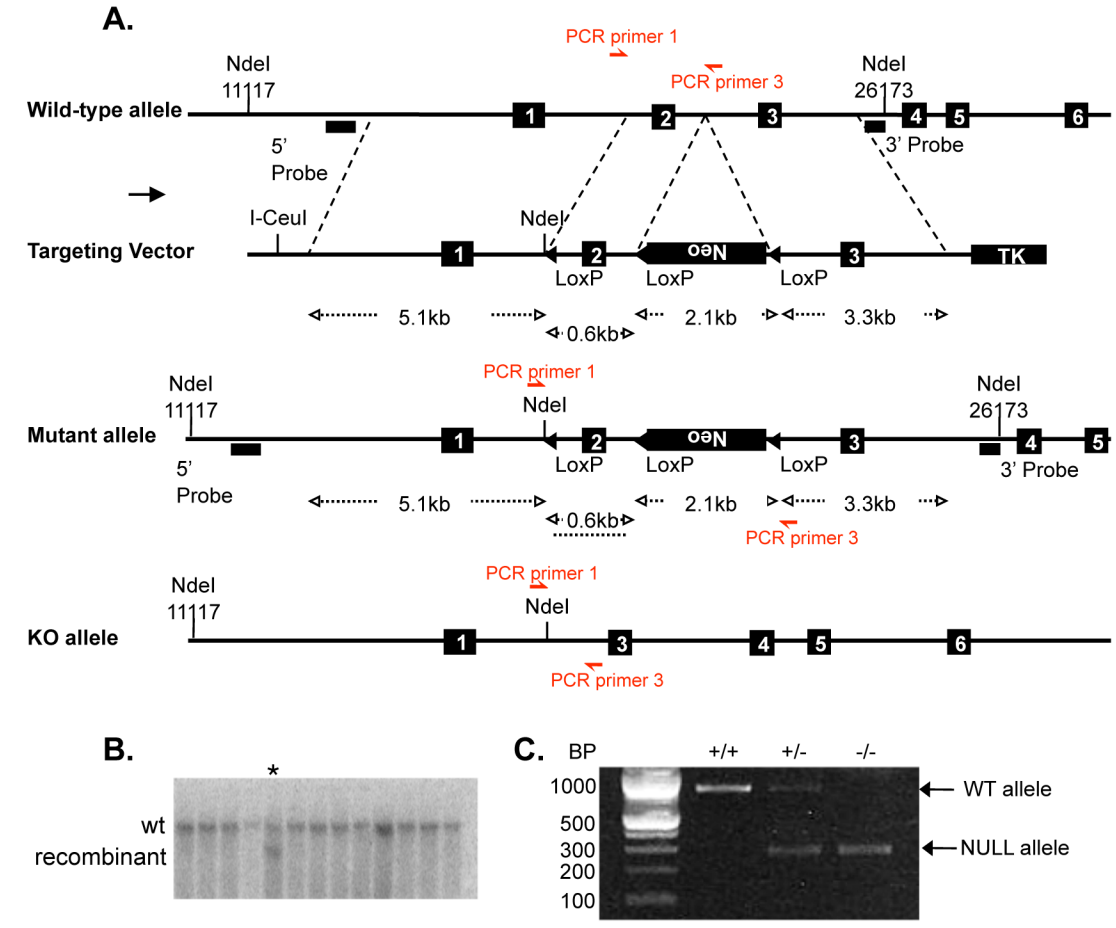
A.
PCR primer 1
NdeI
11117
PCR primer 3
NdeI
26173
Wild-type allele
1
2
3
4
5
6
5'
Probe
3' Probe
I-CeuI
NdeI
Targeting Vector
1
2
Neo
3
TK
LoxP
LoxP
LoxP
5.1kb
0.6kb
2.1kb
3.3kb
PCR primer 1
NdeI
11117
NdeI
26173
Mutant allele
1
2
Neo
3
4
5
5'
Probe
LoxP
LoxP
LoxP
3' Probe
5.1kb
0.6kb
2.1kb
3.3kb
PCR primer 3
PCR primer 1
NdeI
11117
NdeI
KO allele
1
3
4
5
6
PCR primer 3
B.
*
wt
recombinant
C.
BP
+/+
+/-
-/-
1000
500
300
200
100
WT allele
NULL allele

Figure 2

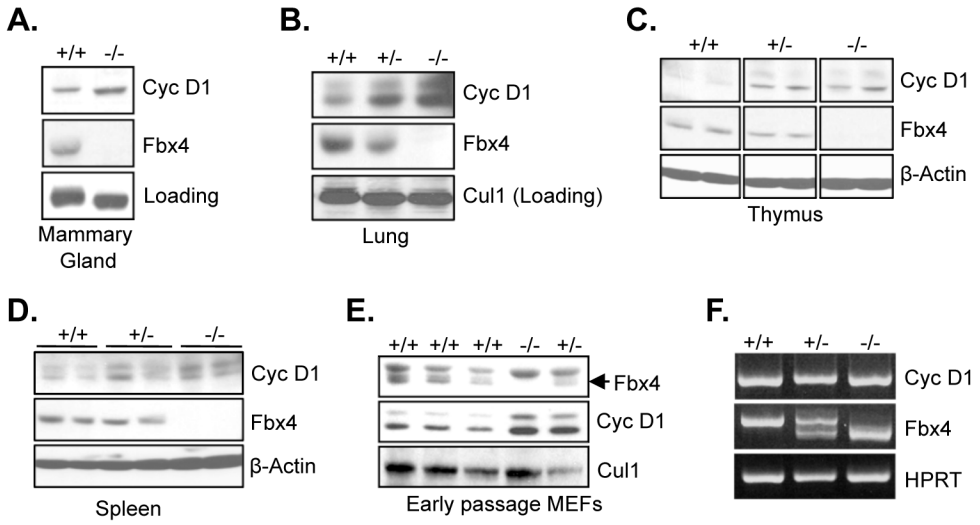
A.
+/+ -/-
Cyc D1
Fbx4
Loading
Mammary Gland
B.
+/+ +/- -/-
Cyc D1
Fbx4
Cul1 (Loading)
Lung
C.
+/+ +/- -/-
Cyc D1
Fbx4
β-Actin
Thymus
D.
+/+ +/- -/-
Cyc D1
Fbx4
β-Actin
Spleen
E.
+/+ +/+ +/+ -/- +/-
Fbx4
Cyc D1
Cul1
Early passage MEFs
F.
+/+ +/- -/-
Cyc D1
Fbx4
HPRT

Figure 3

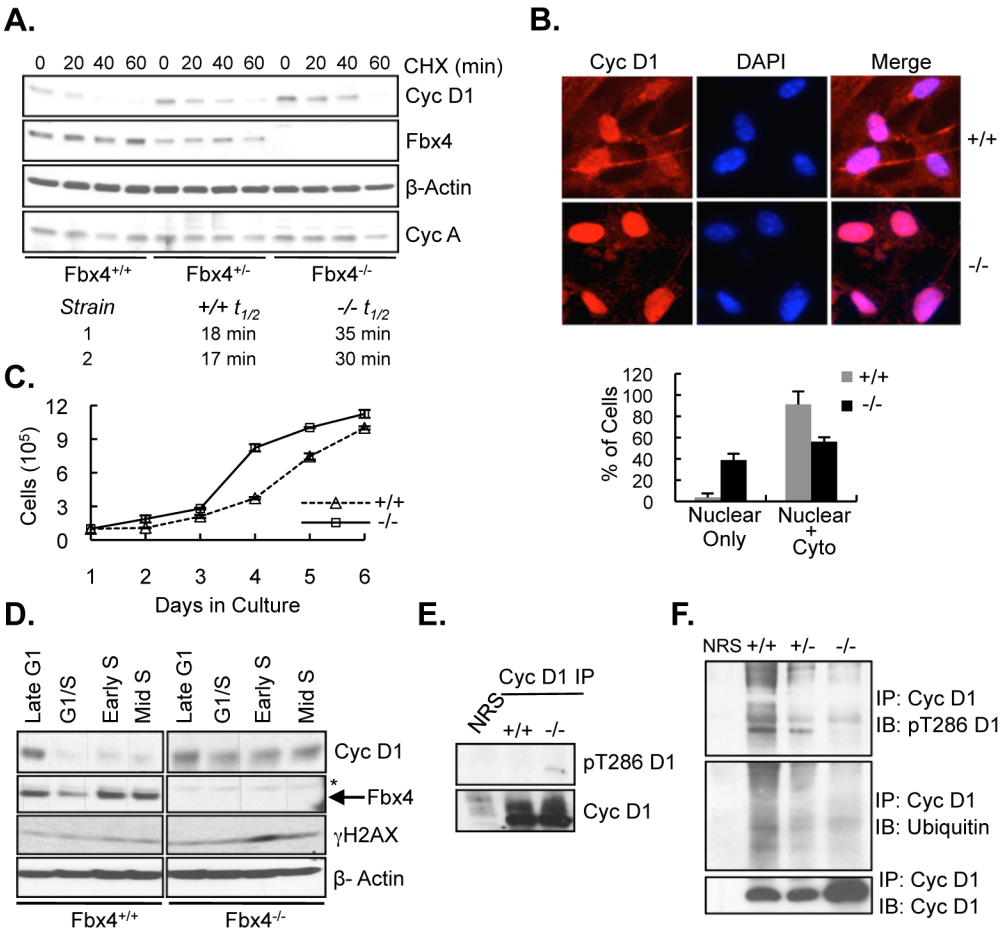
A.
0 20 40 60 0 20 40 60 0 20 40 60 CHX (min)
Cyc D1
Fbx4
β-Actin
Cyc A
Fbx4+/+
Fbx4+/-
Fbx4-/-
Strain
+/+ t1/2
-/- t1/2
1
18 min
35 min
2
17 min
30 min
B.
Cyc D1
DAPI
Merge
+/+
-/-
% of Cells
120
100
80
60
40
20
0
+/+
-/-
Nuclear Only
Nuclear + Cyto
C.
Cells (10^5)
12
9
6
3
0
1 2 3 4 5 6
Days in Culture
+/+
-/-
D.
Late G1
G1/S
Early S
Mid S
Late G1
G1/S
Early S
Mid S
Cyc D1
*
Fbx4
γH2AX
β- Actin
Fbx4+/+
Fbx4-/-
E.
Cyc D1 IP
NRS
+/+ -/-
pT286 D1
Cyc D1
F.
NRS +/+ +/- -/-
IP: Cyc D1
IB: pT286 D1
IP: Cyc D1
IB: Ubiquitin
IP: Cyc D1
IB: Cyc D1

Figure 4

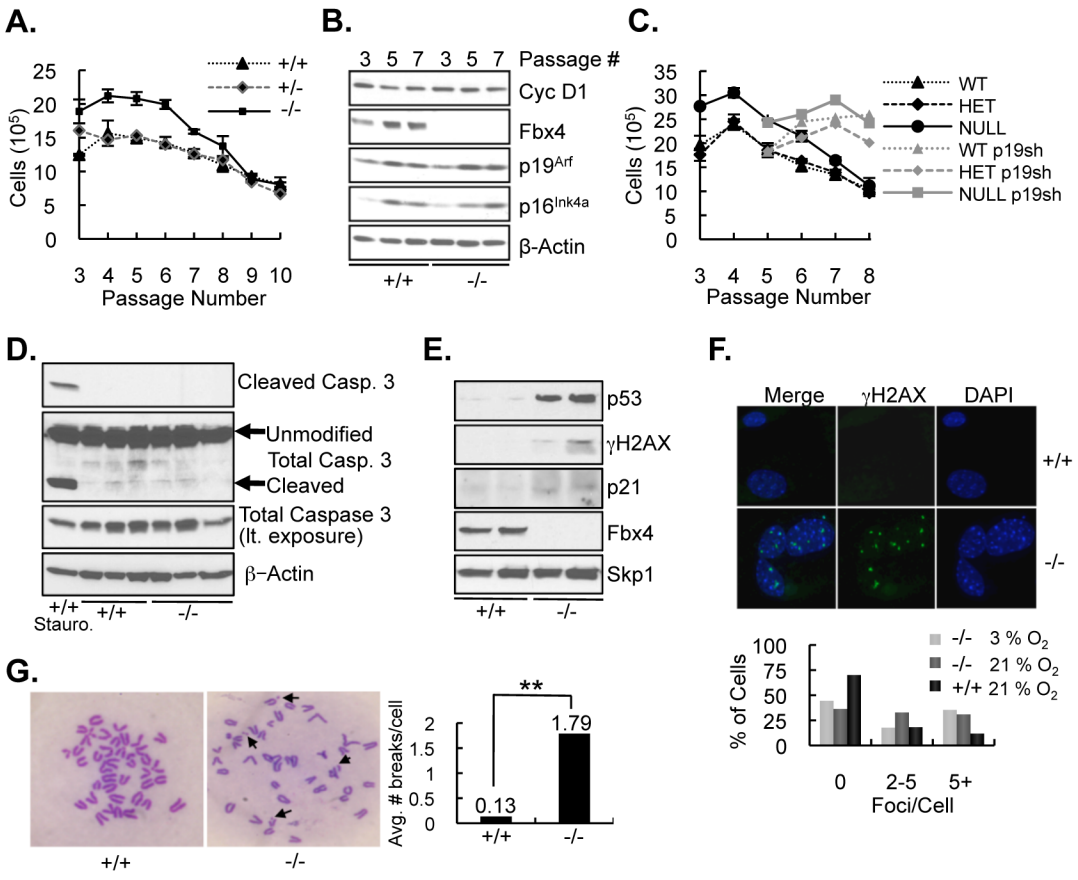
A.
Cells (10^5)
Passage Number
+/+
+/-
-/-
B.
3 5 7 3 5 7 Passage #
Cyc D1
Fbx4
p19Arf
p16Ink4a
β-Actin
+/+
-/-
C.
Cells (10^5)
Passage Number
WT
HET
NULL
WT p19sh
HET p19sh
NULL p19sh
D.
Cleaved Casp. 3
Unmodified
Total Casp. 3
Cleaved
Total Caspase 3
(lt. exposure)
β−Actin
+/+ +/+ -/-
Stauro.
E.
p53
γH2AX
p21
Fbx4
Skp1
+/+ -/-
F.
Merge
γH2AX
DAPI
+/+
-/-
% of Cells
-/- 3 % O2
-/- 21 % O2
+/+ 21 % O2
0 2-5 5+
Foci/Cell
G.
+/+
-/-
Avg. # breaks/cell
**
1.79
0.13
+/+ -/-

Figure 5

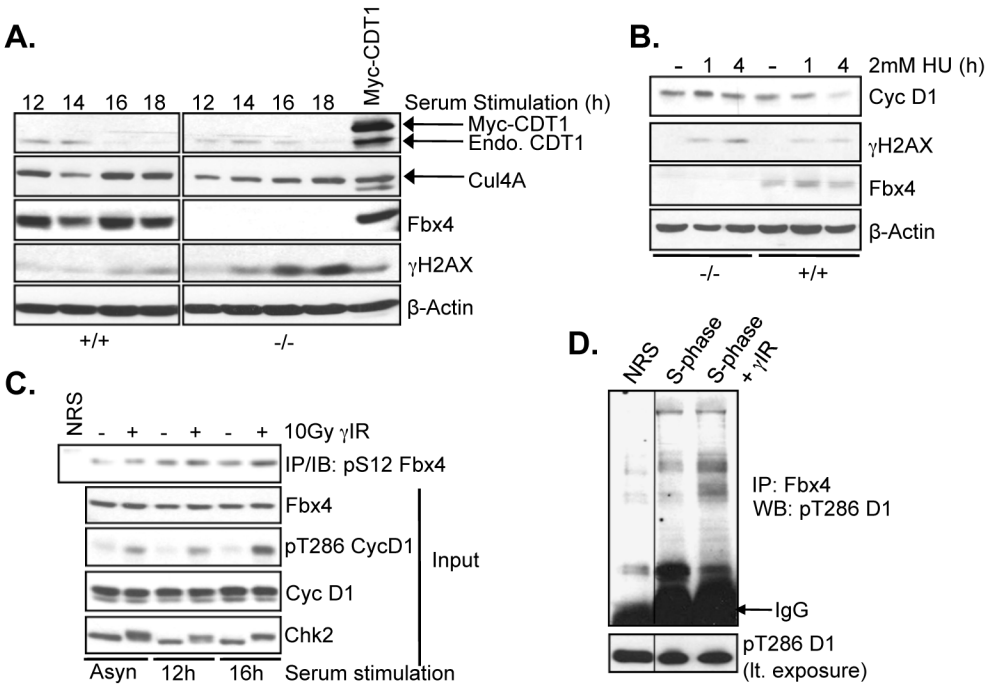
A.
Myc-CDT1
12 14 16 18 12 14 16 18
Serum Stimulation (h)
Myc-CDT1
Endo. CDT1
Cul4A
Fbx4
γH2AX
β-Actin
+/+
-/-
B.
- 1 4 - 1 4 2mM HU (h)
Cyc D1
γH2AX
Fbx4
β-Actin
-/-
+/+
C.
NRS
- + - + - + 10Gy γIR
IP/IB: pS12 Fbx4
Fbx4
pT286 CycD1
Cyc D1
Chk2
Input
Asyn 12h 16h Serum stimulation
D.
NRS
S-phase
S-phase + γIR
IP: Fbx4
WB: pT286 D1
IgG
pT286 D1
(lt. exposure)

Figure 6

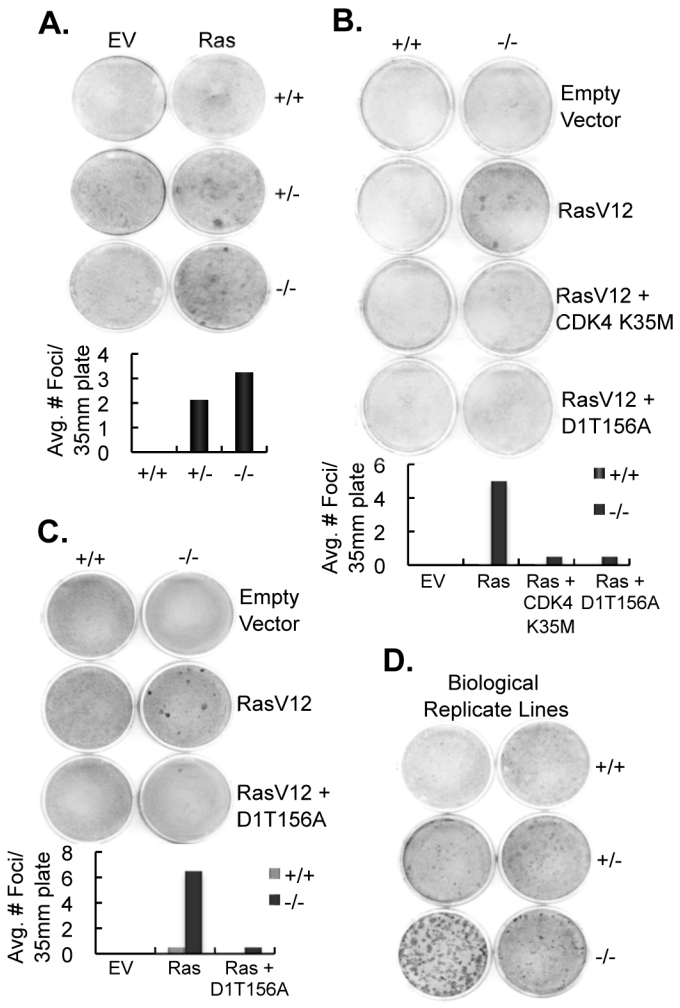
A.
EV
Ras
+/+
+/-
-/-
Avg. # Foci/ 35mm plate
4
3
2
1
0
+/+ +/- -/-
B.
+/+
-/-
Empty Vector
RasV12
RasV12 + CDK4 K35M
RasV12 + D1T156A
Avg. # Foci/ 35mm plate
6
4
2
0
+/+
-/-
EV
Ras
Ras + CDK4 K35M
Ras + D1T156A
C.
+/+
-/-
Empty Vector
RasV12
RasV12 + D1T156A
Avg. # Foci/ 35mm plate
8
6
4
2
0
+/+
-/-
EV
Ras
Ras + D1T156A
D.
Biological Replicate Lines
+/+
+/-
-/-

Figure 7

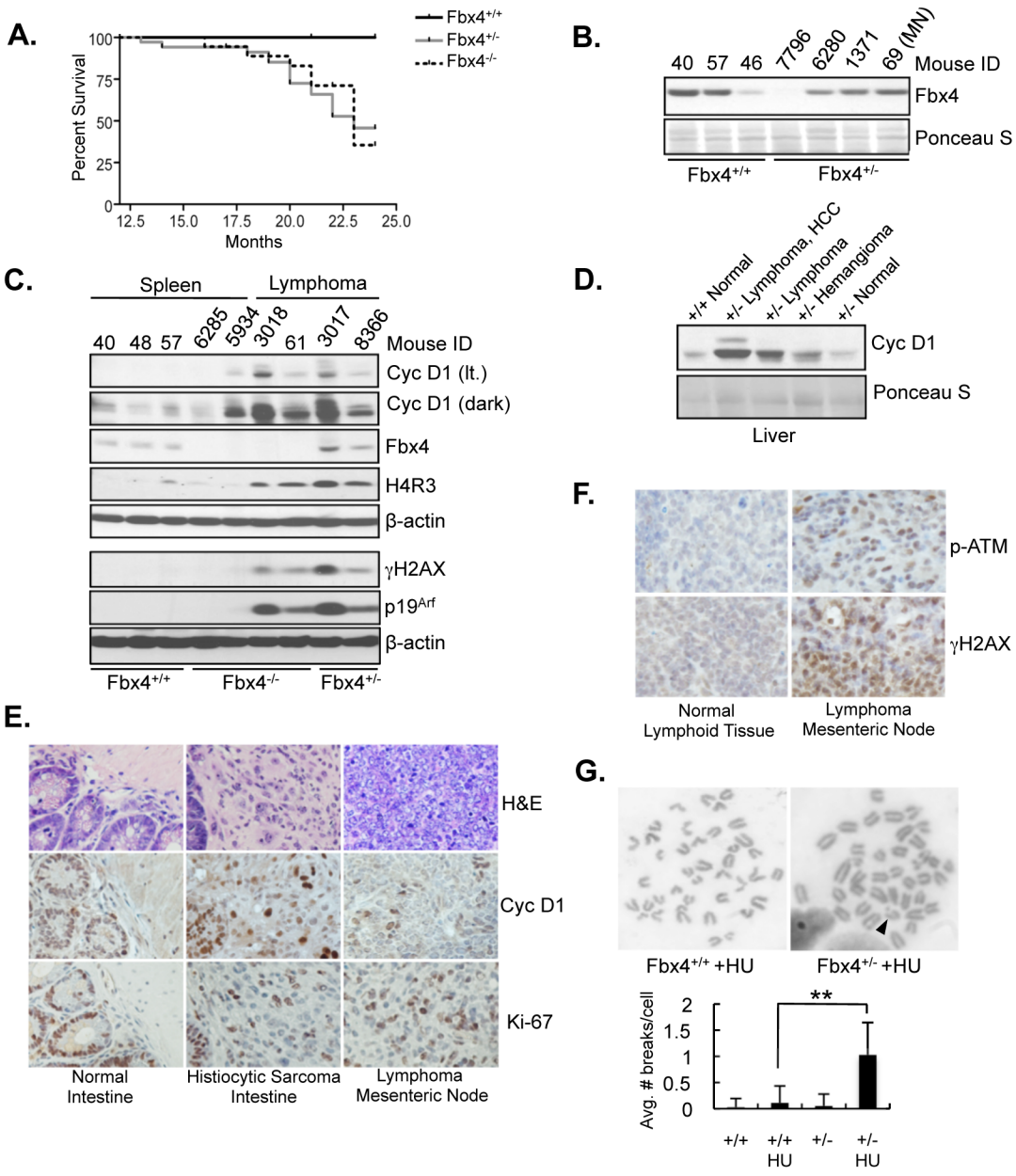
A.
Fbx4+/+
Fbx4+/-
Fbx4-/-
Percent Survival
100
75
50
25
0
12.5
15.0
17.5
20.0
22.5
25.0
Months
B.
40 57 46 7796 6280 1371 69 (MN)
Mouse ID
Fbx4
Ponceau S
Fbx4+/+
Fbx4+/-
C.
Spleen
Lymphoma
40 48 57 6285 5934 3018 61 3017 8366
Mouse ID
Cyc D1 (lt.)
Cyc D1 (dark)
Fbx4
H4R3
β-actin
γH2AX
p19Arf
β-actin
Fbx4+/+
Fbx4-/-
Fbx4+/-
D.
+/+ Normal
+/- Lymphoma, HCC
+/- Lymphoma
+/- Hemangioma
+/- Normal
Cyc D1
Ponceau S
Liver
E.
H&E
Cyc D1
Ki-67
Normal Intestine
Histiocytic Sarcoma Intestine
Lymphoma Mesenteric Node
F.
p-ATM
γH2AX
Normal Lymphoid Tissue
Lymphoma Mesenteric Node
G.
Fbx4+/+ +HU
Fbx4+/- +HU
**
Avg. # breaks/cell
2
1.5
1
0.5
0
+/+
+/+ HU
+/-
+/- HU

Table 1

Table I. Pathology observed in $Fbx4^{+/-}$ and $Fbx4^{-/-}$ mice.

Pathology	No. of Mice	Incidence
Lymphoblastic Lymphoma (Spleen, Thymus, Mesenteric Node, Liver, Intestine)	18/47	38.3%
Extramedullary Hematopoiesis/Intense Myeloid Proliferation (Spleen, Liver)	11/47	23.4%
Hemangioma/Angioinvasive Tumor (Liver, Lung)	3/47	6.4%
Dendritic Cell Tumor (Spleen, Thymus)/Histiocytic Sarcoma (Intestine)	3/47	6.4%
Early Myeloid Tumor	1/47	2.1%
Mammary Carcinoma	1/47	2.1%
Uterine Tumor	1/47	2.1%

Table 1. Summary of pathology observed in $Fbx4^{+/-}$ and $Fbx4^{-/-}$ mice. $Fbx4^{+/-}$ and $Fbx4^{-/-}$ mice included as events in the Kaplan-Meier survival analysis frequently develop large cell lymphoblastic lymphomas involving the mesenteric lymph node, spleen, thymus, Peyer's patches of the intestine, and liver. A large percentage of mice also exhibit extramedullary hematopoiesis (EMH) and intense myeloid proliferation in the spleen and less frequently, liver. This is also associated with early myeloid tumor formation. Less commonly observed malignancies include dendritic cell/histiocytic sarcomas, hemangioma, uterine tumor, and mammary carcinoma. Analysis of several mice independent of the Kaplan-Meier cohort also revealed an additional case of intestinal histiocytic sarcoma and a case of hepatocellular carcinoma.

Cancer Cell
Article

Nuclear Cyclin D1/CDK4 Kinase Regulates *CUL4* Expression and Triggers Neoplastic Growth via Activation of the PRMT5 Methyltransferase

Priya Aggarwal,[1,5] Laura Pontano Vaites,[1,5] Jong Kyong Kim,[1] Hestia Mellert,[2] Buddha Gurung,[1] Hiroshi Nakagawa,[3] Meenhard Herlyn,[4] Xianxin Hua,[1] Anil K. Rustgi,[3] Steven B. McMahon,[2] and J. Alan Diehl[1,*]
[1]Abramson Family Cancer Research Institute, Department of Cancer Biology, Abramson Cancer Center, University of Pennsylvania, Philadelphia, PA 19104, USA
[2]Department of Cancer Biology, Thomas Jefferson University, Philadelphia, PA 19107, USA
[3]Division of Gastroenterology, Department of Medicine and Abramson Cancer Center University of Pennsylvania University of Pennsylvania, Philadelphia, PA 19104, USA
[4]The Wistar Institute, Philadelphia, PA 19104, USA
[5]These authors contributed equally to this work
*Correspondence: adiehl@mail.med.upenn.edu
DOI 10.1016/j.ccr.2010.08.012

SUMMARY

Cyclin D1 elicits transcriptional effects through inactivation of the retinoblastoma protein and direct association with transcriptional regulators. The current work reveals a molecular relationship between cyclin D1/CDK4 kinase and protein arginine methyltransferase 5 (PRMT5), an enzyme associated with histone methylation and transcriptional repression. Primary tumors of a mouse lymphoma model exhibit increased PRMT5 methyltransferase activity and histone arginine methylation. Analyses demonstrate that MEP50, a PRMT5 coregulatory factor, is a CDK4 substrate, and phosphorylation increases PRMT5/MEP50 activity. Increased PRMT5 activity mediates key events associated with cyclin D1-dependent neoplastic growth, including *CUL4* repression, CDT1 overexpression, and DNA rereplication. Importantly, human cancers harboring mutations in Fbx4, the cyclin D1 E3 ligase, exhibit nuclear cyclin D1 accumulation and increased PRMT5 activity.

INTRODUCTION

Cyclin D1, the allosteric regulator of CDK4 and CDK6, is an integral mediator of growth factor-dependent G1-phase progression. Growth factor stimulation induces cyclin D1 expression, association with CDK4, and nuclear accumulation during mid-G1; active cyclin D1/CDK4 kinase catalyzes phosphorylation-dependent inactivation of the retinoblastoma (RB) family proteins (Diehl, 2002). Following the G1/S transition, cyclin D1 accumulation is opposed by Pro287-directed phosphorylation of threonine-286 (T286) by glycogen synthase kinase 3β (GSK3β), which promotes its nuclear export (Alt et al., 2000). Cytoplasmic, phosphorylated cyclin D1 is polyubiquitylated by SCF^{Fbx4} and degraded by the 26S proteasome (Lin et al., 2006).

Overexpression of cyclin D1 occurs in numerous human malignancies, including carcinomas of the breast, esophagus, colon, and lung (Bani-Hani et al., 2000; Bartkova et al., 1994a; Bartkova et al., 1995; Bartkova et al., 1994b; Gillett et al., 1994; Herman et al., 1995; Hibberts et al., 1999; Hosokawa and Arnold, 1998; Hosokawa et al., 1999; Jin et al., 2001). Although overexpression of cyclin D1 is often observed, overexpression per se is insufficient to drive spontaneous transformation. The primary cellular mechanism that restricts cyclin D1/CDK4 activity is cytoplasmic, ubiquitin-mediated degradation

Significance

Cyclin D1 contributes to cell growth through phosphorylation of the retinoblastoma protein and direct association with transcriptional regulators. Our work demonstrates that direct regulation of critical target genes associated with neoplastic transformation depends on cyclin D1 activation of CDK4. The identification of a CDK4 substrate that contributes to epigenetic regulation of target genes associated with cancer establishes a paradigm whereby cyclin D1 regulation of gene expression occurs independently of RB yet remains kinase dependent. The association of cyclin D1 with transcriptional repression in concert with the repressive nature of PRMT5-dependent histone methylation supports a model wherein PRMT5/MEP50 is one key effector of cyclin D1-dependent gene expression during neoplastic growth.

of cyclin D1 during S-phase. Mutations that disrupt this event directly contribute to neoplastic growth (Aggarwal et al., 2007; Alt et al., 2000; Barbash et al., 2008; Benzeno et al., 2006; Lu et al., 2003). Specifically, inhibition of cyclin D1 proteolysis during S-phase via mutations within the cyclin D1 degron or inactivation of the cyclin D1 E3 ligase, Fbx4, triggers constitutive nuclear accumulation of active cyclin D1/CDK4 complexes, which, in turn, disrupt temporal regulation of DNA replication, thereby contributing to neoplastic growth. The disruption of S-phase fidelity reflects accumulation of the replication-licensing protein CDT1. Inappropriate CDT1 stabilization is a result of nuclear cyclin D1/CDK4-dependent repression of *CUL4A* and *CUL4B*, encoding scaffolding proteins for the E3 ligase that directs CDT1 degradation during S-phase (Aggarwal et al., 2007).

Numerous previous studies have linked cyclin D1 with transcriptional repression. The current model focuses on an intrinsic capacity of cyclin D1 to associate directly with transcriptional regulators and either interfere with the recruitment of cofactors that direct gene repression or, conversely, facilitate coactivator recruitment as observed in the collaboration between cAMP signaling and cyclin D1 in the activation of estrogen receptor (ER)-mediated transcription in mammary epithelial cells (Lamb et al., 2000). The strongest evidence for cyclin D1 directly contributing to the regulation of gene expression stems from recent work utilizing genome-wide chromatin immune precipitation to identify promoters occupied by cyclin D1 (Bienvenu et al., 2010).

A common theme throughout previous studies is that cyclin D1 modulates gene expression in a kinase-independent manner. However, transcriptional repression of *CUL4A* and *CUL4B* by cyclin D1 requires S-phase accumulation of catalytically active cyclin D1/CDK4 (Aggarwal et al., 2007). The current study dissects the molecular mechanism of *CUL4A/B* transcriptional regulation by cyclin D1 and its contribution to nuclear cyclin D1-driven neoplastic growth.

RESULTS

Association of the PRMT5/MEP50 Methyltransferase with Cyclin D1T286A/CDK4

To decipher mechanisms of nuclear cyclin D1-driven neoplasia, we immunopurified cyclin D1T286A complexes from tumors derived from Eμ-D1T286A transgenic mice (Gladden et al., 2006) and identified copurifying proteins by mass spectrometry (see Figure S1A available online). Given previous reports linking cyclin D1 with transcriptional repression, we were intrigued by copurification of PRMT5, a Type II methyltransferase, along with MEP50, a WD40 repeat-containing protein that contributes to PRMT5 activity and substrate recruitment (peptides recovered are shown in Table S1; Krause et al., 2007). Coprecipitation of cyclin D1T286A, CDK4, MEP50, and PRMT5 from B cell tumors confirmed the interaction (Figures 1A and 1B). To ascertain the existence of this complex in human cancer cells, we used TE3 and TE7 cell lines that harbor cyclin D1P287A (Benzeno et al., 2006). Cyclin D1P287A is refractory to GSK3β-dependent phosphorylation and is stabilized in the nucleus, analogous to D1T286A. Consistent with the above results, we also observed coprecipitation of cyclin D1P287A along with MEP50, PRMT5, and CDK4 (Figure 1C).

Association of cyclin D1T286A with PRMT5, in concert with previous work demonstrating that cyclin D1T286A reduces *CUL4A/B* expression in a CDK4-dependent manner (Aggarwal et al., 2007), suggested a potential regulatory relationship involving cyclin D1T286A and chromatin-modifying proteins. To interrogate this putative relationship, we coexpressed Myc-PRMT5 together with CDK4 and either wild-type cyclin D1 or D1T286A in HeLa cells. Following synchronization at the G1/S boundary and release into S-phase, complexes were immune precipitated, and associated proteins were identified by immunoblot. Cyclin D1T286A was enriched in PRMT5 complexes at the G1/S boundary and declined as cells progressed through S-phase (Figure 1D; Figure S1B). In contrast, low levels of wild-type cyclin D1 were associated with PRMT5, with no obvious enrichment. The reduced binding of wild-type cyclin D1 reflects both its low abundance, due to proteolysis during S-phase, and cytoplasmic localization of the remaining protein (Alt et al., 2000; Barbash et al., 2008).

To determine whether known components of chromatin-remodeling complexes were also present in the cyclin D1T286A-PRMT5 complex, we performed a two-step affinity purification of this complex. Initially, Flag-D1T286A-containing complexes were collected from pooled tumor lysates by M2-affinity chromatography, which was used to isolate flag-tagged cyclin D1. Complexes were eluted with flag peptide then reprecipitated with PRMT5 antibodies. In addition to the expected components (cyclin D1T286A, CDK4, PRMT5, and MEP50) we also noted Brg1 (Figure 1E). Importantly, these complexes do not contain RB, PRMT5-related PRMT1 and PRMT7, mSin3a (a component of large multisubunit histone deacetylase [HDAC] corepressor complexes), or Mi2 (a nucleosome remodeling and HDAC complex component) (Figure 1E). This result reveals the existence of a cyclin D1T286A, CDK4, MEP50, PRMT5, and Brg1 complex. Consistently, we also noted coprecipitation of Brg1 with endogenous cyclin D1P287A in TE3 and TE7 cells (Figure 1C). Consistently, size exclusion chromatography revealed cofractionation of cyclin D1T286A, CDK4, PRMT5, MEP50, and Brg1 in murine lymphomas (Figure S1C).

PRMT5/MEP50 Mediates Cyclin D1T286A/CDK4-Dependent *CUL4A/B* Loss and CDT1 Stabilization

Because PRMT5-dependent dimethylation of histone H3 arginine 8 (H3R8) and histone H4 arginine 3 (H4R3) is associated with transcriptional repression (Pal et al., 2004), we considered whether PRMT5 would mediate cyclin D1T286A/CDK4-dependent repression of *CUL4A/B*. We first used the general methyltransferase inhibitor 5′ Deoxy-5″-methyl-thioadenosine (MTA; Hou et al., 2008; Iwasaki and Yada, 2007) following identification of a concentration that inhibited H4R3 methylation but not H3K4 methylation (Figure 2A). As previously observed, expression of catalytically active cyclin D1T286A/CDK4 resulted in the maintenance of CDT1 and loss of CUL4A/B proteins and mRNAs specifically during S-phase (Figures 2B–2D). Treatment with 100 μM MTA restored CUL4A/B proteins and mRNAs (Figures 2B–2D) and triggered CDT1 degradation during S-phase (Figure 2B). A similar restoration of *CUL4A/B* was observed with another PRMT inhibitor, AMI-1 (Cheng et al., 2004) (Figures S2A–S2D).

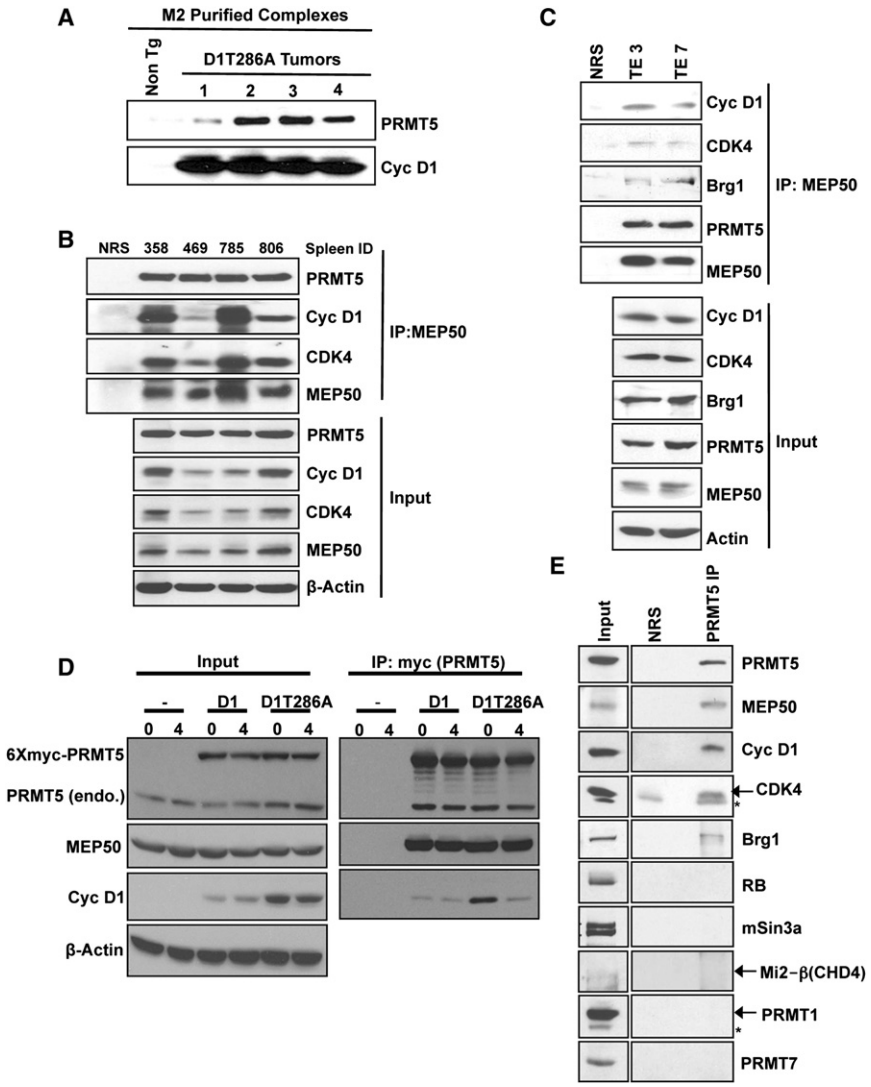

Figure 1. Identification of Cyclin D1T286A/PRMT5/MEP50 Complexes

(A) M2 (anti-Flag) purified complexes from Eμ-D1T286A (Flag epitope) transgenic tumors and nontransgenic spleens were blotted for PRMT5 and cyclin D1.

(B) MEP50 immunoprecipitates (IP, 1 mg whole-cell lysate input) prepared from Eμ-D1T286A transgenic tumors were immunoblotted as indicated.

(C) MEP50 IP (1.5mg whole cell lysate input) from human esophageal cancer cell lines TE3 and TE7 were immunoblotted as indicated (top panel). Input lysates have been shown in the bottom panel.

(D) HeLa cells transfected with either wild-type cyclin D1 or D1T286A along with myc-PRMT5 and CDK4 were synchronized with aphidicolin. Cells were collected at 0 hr (G1/S boundary) and 4 hr (S-phase) after release. Myc-PRMT5 was pulled down with myc antibody (1 mg whole cell lysate input) and immunoblotted as indicated (right panel); input lysates are shown in left panel.

(E) Cyclin D1/CDK4 complexes were isolated from Eμ-D1T286A lymphomas using M2-agarose followed by elution with Flag peptide. Eluted complexes were immunoprecipitated with normal rabbit serum (NRS) or PRMT5 antibody; 300 μg of eluted complex served as input in NRS or PRMT5 IP, and western blot analysis was performed as indicated. See also Figure S1 and Table S1.

As an independent assessment of PRMT5 function, we utilized siRNA directed at PRMT5 or MEP50. Knockdown of PRMT5 (Figures 2E, 2G, and 2H) or MEP50 (Figure S2E) restored expression of CUL4A/B and CDT1 loss during S-phase. Knockdown of PRMT5 also reduced H4R3 and H3R8 methylation but did not change levels of PRMT1, 2, and 7 (Figure 2E). We confirmed previous observations that regulation of CUL4 and CDT1 requires the kinase activity of CDK4 given that expression of a kinase defective mutant, CDK4(K35M), does not support cyclin D1T286A-dependent CUL4 loss and eliminates the impact of PRMT5 knockdown (Figure 2F). Further supporting a role for PRMT5 activity downstream of cyclin D1, esophageal cancer cells harboring the mutant cyclin D1 P287A exhibited increased CDT1, decreased CUL4A, and increased H4R3 methylation compared to cells with wild-type cyclin D1 (Figure S2F).

Because attenuation of PRMT5 relieves *CUL4* repression, we questioned whether cyclin D1T286A regulates HDAC activity, contributing to *CUL4* repression. Synchronized HeLa cells were treated with the HDAC inhibitors sodium butyrate, trichostatin A, and nicotinamide; each inhibitor increased *CUL4* expression independently of cyclin D1T286A (Figures S2G and S2H). Furthermore, acetylation of histone H3 and H4 within the *CUL4A* promoter (Figure S2I) and *CUL4B* promoter (data not shown) was not influenced by cyclin D1T286A, suggesting that HDAC activity is not coordinately regulated with histone arginine methylation by cyclin D1T286A/CDK4 at the *CUL4* promoters.

Cyclin D1T286A/CDK4 Kinase Directs Increased PRMT5 Activity and PRMT5-Dependent Methylation of *CUL4* Promoters

If PRMT5 mediates the action of cyclin D1T286A/CDK4 in vivo, we reasoned that increased H3R8 dimethylation, a PRMT5-specific mark (Pal et al., 2004), should be apparent in tumors derived from Eμ-D1T286A mice. Methylated H3R8 was elevated in tumors compared to nontransgenic controls (Figure 3A and Figure S3A; see Figure S3C for H3R8 antibody specificity). To determine whether increased methylation of histones reflected increased PRMT5 activity, we assessed methyltransferase activity of PRMT5 immunopurified from control or tumor-burden spleens and found that four of six tumors exhibited an increase in PRMT5 activity (Figure 3B). Although PRMT5 levels are increased in cyclin D1T286A tumors, it does not appear sufficient to account for the dramatic increase in PRMT5 catalysis

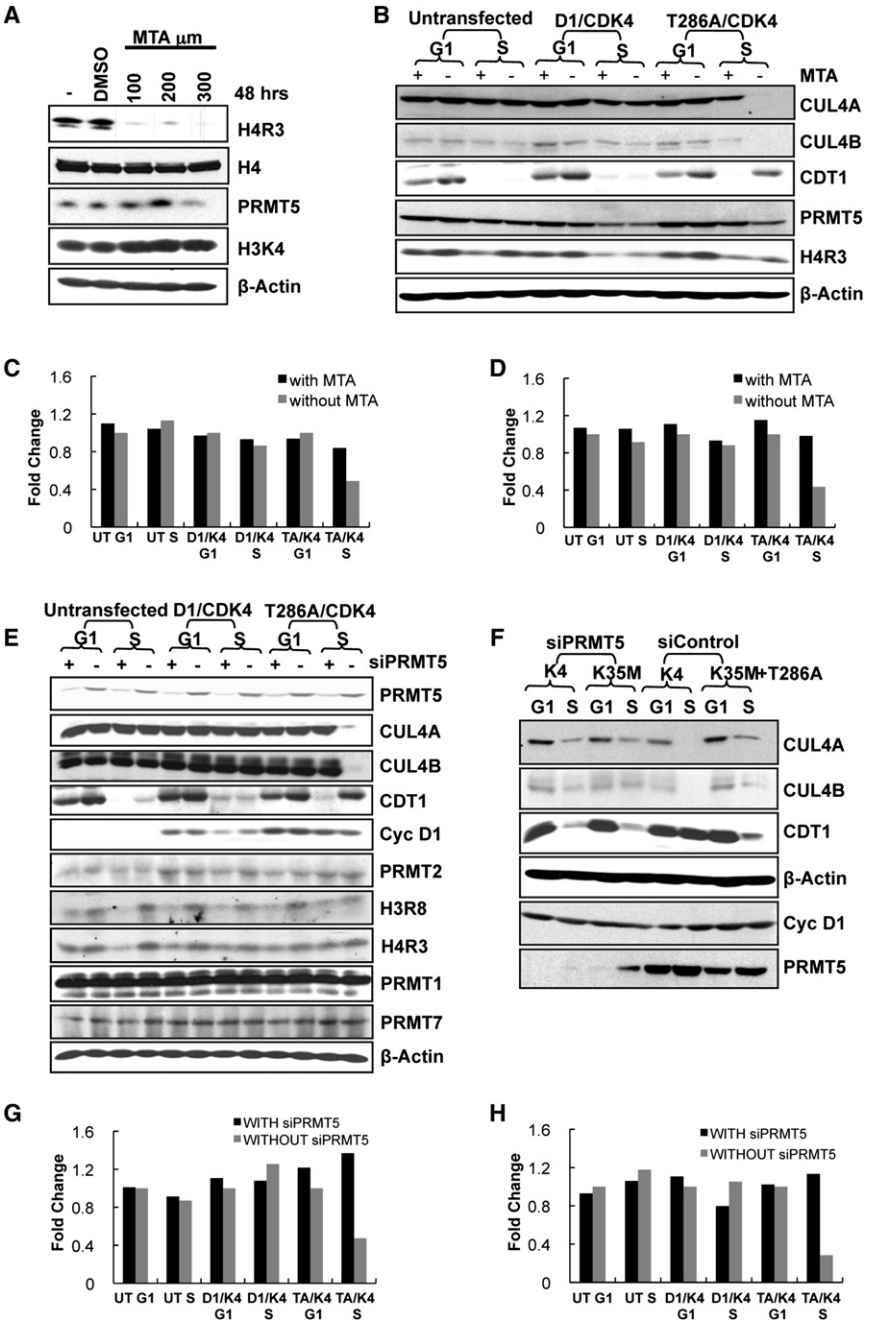

Figure 2. PRMT5/MEP50 Mediates Cyclin D1T286A/CDK4-Dependent *CUL4* Repression and CDT1 Stabilization

(A) HeLa cells were treated with MTA (5′ Deoxy-5″-methyl-thioadenosine) with concentrations ranging from 100 to 300 μM for 48 hr or vehicle DMSO. The cells were analyzed by western blotting as indicated.

(B) HeLa cells cultured for 24 hr in the absence or presence of 100 μM MTA were transfected with vectors encoding cyclin D1 or D1T286A and CDK4. Twenty-four hours after transfection, cells were synchronized with nocodazole for 16–18 hr; mitotic cells were then separated in two dishes. One was harvested 8 hr after release (G1-phase). Hydroxyurea was added to the second after release and harvested at 14 hr to obtain cells in S-phase; lysates were subjected to immunoblot as indicated.

(C and D) RNA was collected from HeLa cells treated as in (B). The bars illustrate *CUL4A* (C) and *CUL4B* (D) mRNA levels with MTA treatment (first bar) and without MTA treatment (second bar) as analyzed by real-time PCR. One representative experiment of three biological independent experiments is presented.

(E) HeLa cells were treated with or without siPRMT5 then transfected with wild-type cyclin D1 or D1T286A plasmids along with CDK4. Cells were synchronized as in (B) and were immunoblotted as indicated.

(F) HeLa cells were treated with siPRMT5 or si control for 24 hr, followed by transfection with cyclin D1T286A along with CDK4 or kinase dead CDK4(K35M) plasmids. Cells were synchronized as in (B), and lysates were immunoblotted as indicated.

(G and H) Same as (C) and (D), except that cells were analyzed with and without siPRMT5 treatment. See also Figure S2.

observed. We also observed increased methylation of recombinant H3R8 in vitro (Figure S3B). To more directly determine whether this increase reflects the action of cyclin D1T286A/CDK4, we reconstituted this pathway in HeLa cells. Consistently, PRMT5 isolated from S-phase cells expressing cyclin D1T286A exhibited enhanced methyltransferase activity; a small but significant increase was also observed in cells overexpressing wild-type cyclin D1/CDK4 (Figure 3C).

Given the increase in total H4R3/H3R8 methylation, we determined whether there was an increase in H4R3/H3R8 methylation on the proximal *CUL4A/B* promoter regions by ChIP using antibodies detecting dimethylated H4R3 and dimethylated H3R8 (see Figure S3D for primer design). We observed an ~2- to 3-fold increase in methylation of both H4R3 and H3R8 at the proximal promoter regions (~500 bp upstream of the first coding exon) of *CUL4A* (Figure 3D) and *CUL4B* (Figure S3E) in the presence of cyclin D1T286A/CDK4 as compared to cyclin D1/CDK4 or untransfected controls in S-phase HeLa cells. No enrichment was detected with primers directed to regions corresponding to 1000 bp upstream (data not shown) or ~5000 bp upstream of first coding exon of *CUL4A/B* (control/blue bars Figures 3D; Figure S3E). Using PRMT5-specific antibodies for ChIP, we noted PRMT5 occupancy of the same region of the *CUL4* promoters (Figure S3F). Critically, siRNA-mediated knockdown of PRMT5 resulted in significant attenuation of cyclin D1T286A/CDK4-dependent H4R3/H3R8 methylation at *CUL4A/B* promoter regions during S-phase (Figure 3E). In agreement with cyclin D1T286A directly contributing to increased PRMT5 activity, cyclin D1T286A

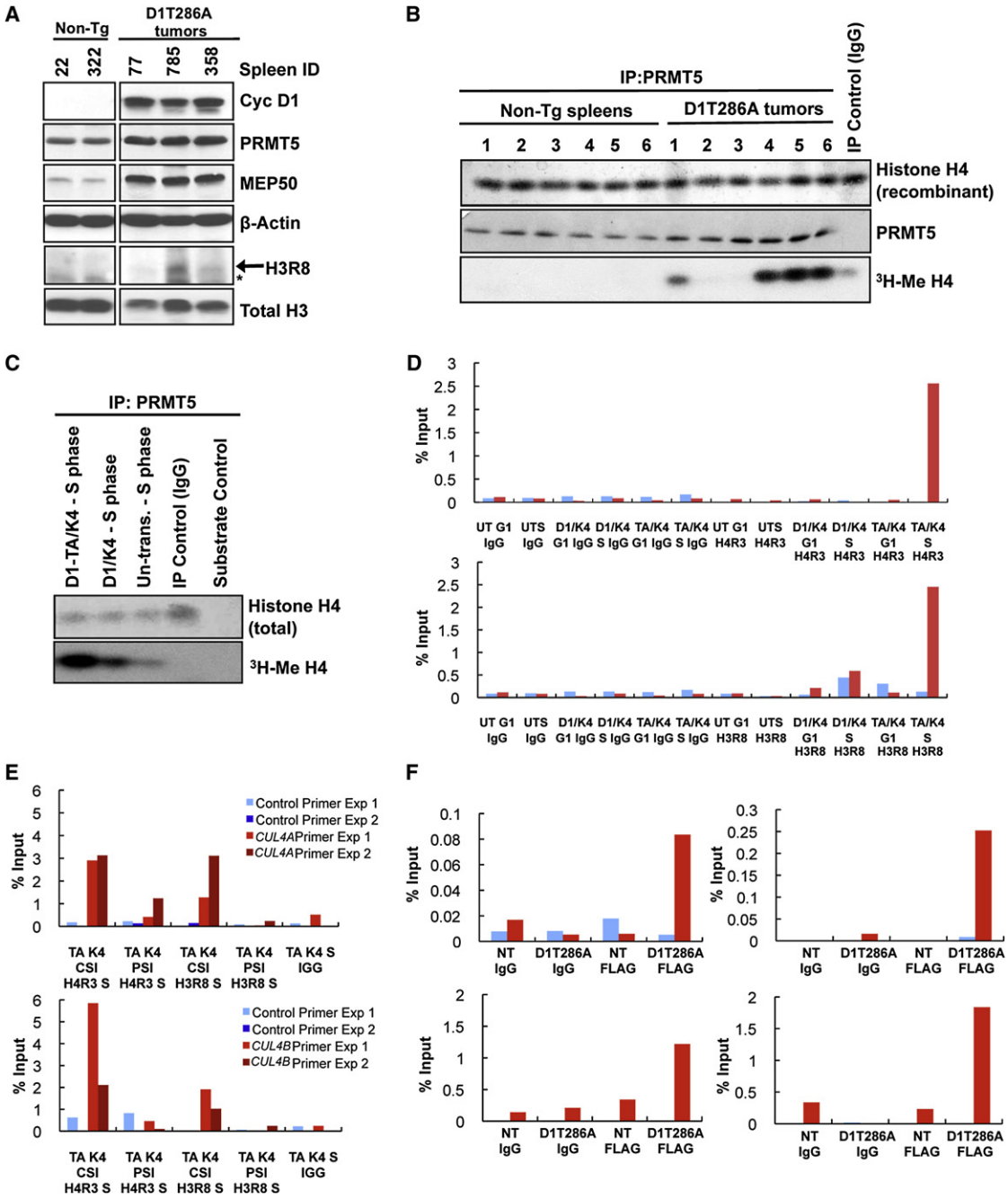

Figure 3. Cyclin D1T286A/CDK4 Activity Increases PRMT5 Methyltransferase Activity In Vivo

(A) Nontransgenic spleen or cyclin D1T286A-driven splenic lymphoma lysates were immunoblotted as indicated.

(B) Methyltransferase activity of tumor-derived PRMT5 using recombinant histone H4 as the substrate.

(C) Same as (B), except that PRMT5 complexes were immunopurified from HeLa cells transfected with the indicated plasmids and synchronized in S-phase.

(D–F) ChIP primer sets (1, 2, and 3) were designed to span 1000–2000 bp upstream of the first coding exon of either *CUL4A* or *CUL4B*, respectively (primer design, Figure S3D). Primer set 3 was used for both *CUL4A* and *CUL4B* ChIP assays. Control primer sets were designed ~5000 bp upstream of first coding exon of *CUL4A/B*. The *CUL4A/B* promoter primer (red bar) and control primer (blue bar) are displayed in all graphs. ChIP was performed for *CUL4A* (Figure 3D) and *CUL4B* (Figure S3E) with antibodies directed to dimethyl H4R3 (Figure 3D, top panel), H3R8 (Figure 3D, bottom panel; Figure S3E, right panel), or normal mouse IgG (first 6 bars of each graph), on chromatin prepared from synchronized HeLa cells expressing wild-type cyclin D1/CDK4, D1T286A/CDK4, or untransfected cells. DNA-protein immunoprecipitates and 5% of input chromatin were analyzed by qPCR for both *CUL4A* and *CUL4B* promoter regions. PCR values represent percentage of input. One representative experiment of three biological independent experiments is presented.

(E) PRMT5 knockdown attenuates methylation of H4R3 and H3R8 of *CUL4A* (top graph) and *CUL4B* (bottom graph) promoter regions. ChIP was performed using dimethyl specific H4R3 and H3R8 antibodies as described in (D); two representative experiments are shown.

(F) Detection of cyclin D1T286A on the *Cul4A/B* proximal promoter by Flag ChIP from Eμ-D1T286A tumors. Two independent experiments are shown. See also Figure S3.

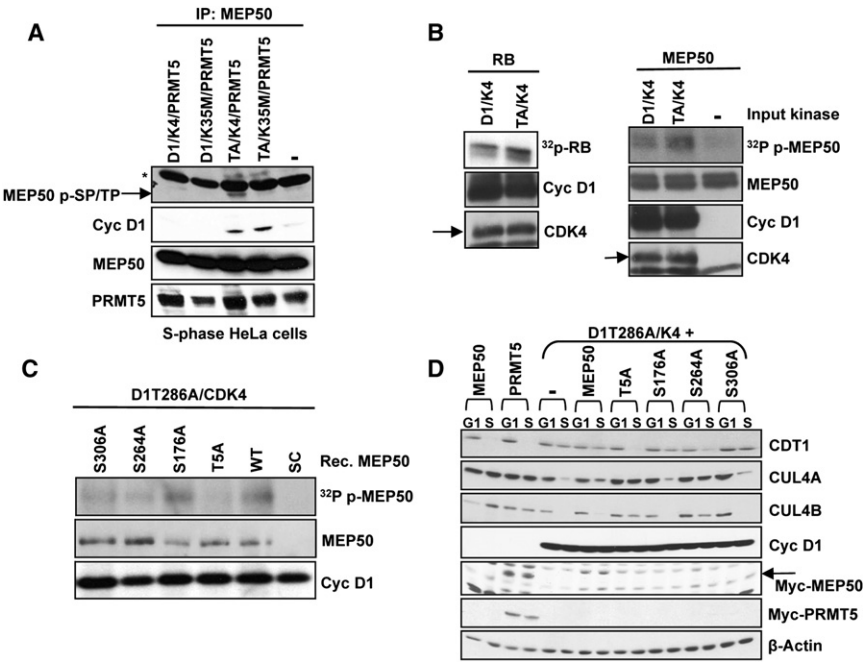

Figure 4. Cyclin D1/CDK4 Kinase Phosphorylates MEP50 In Vitro and In Vivo

(A) MEP50 was precipitated from HeLa cells transfected with vectors encoding cyclin D1, D1T286A along with either CDK4 or kinase dead CDK4 (K35M) and synchronized in S-phase by sequential nocodazole and HU treatment. MEP50 phosphorylation was assessed using a commercially available phospho-SP/TP antibody. The arrow indicates the mobility of phospho-MEP50, which migrates faster than the asterisk-indicated nonspecific immunoreactive band. Total MEP50, PRMT5, and cyclin D1 present in immune complexes were assessed with appropriate antibodies.

(B) Phosphorylation of recombinant MEP50 or RB by cyclin D1/CDK4 or D1T286A/CDK4. Substrate phosphorylation was assessed by SDS-PAGE followed by autoradiography.

(C) Cyclin D1T286A/CDK4 phosphorylation of MEP50 at Thr-5, Ser-264, and Ser-306 in vitro.

(D) Acute expression of MEP50 mutants Thr-5A and Ser-264A inhibit cyclin D1T286A/CDK4-dependent repression of CUL4 and CDT1 stabilization. See also Figure S4.

occupancy of both *Cul4A/B* promoters was observed in cyclin D1T286A-expressing primary murine lymphoma cells (Figure 3F). Consistent with the presence of Brg1 in the cyclin D1T286A/PRMT5 complex, Brg1 also occupies the *Cul4A* and *Cul4B* promoters (Figure S3G).

Phosphorylation of MEP50 by Cyclin D1T286A/CDK4 In Vitro and In Vivo

We next considered whether either MEP50 or PRMT5 might be a cyclin D1/CDK4 substrate. PRMT5/MEP50 complexes were precipitated from HeLa cells expressing cyclin D1 or cyclin D1T286A along with either CDK4 or CDK4(K35M) with a MEP50 antibody. Upon immunoblotting with an antibody detecting phosphorylated serine or threonine when either residue is followed by a proline, we noted a band in cells expressing cyclin D1T286A/CDK4 that migrated with the expected mobility of MEP50 (Figure 4A, noted by arrow). No such band was apparent in cyclin D1-expressing cells or in cyclin D1T286A/CDK4(K35M)-expressing cells. In addition, we did not detect any apparent p-SP/TP signal corresponding to PRMT5.

MEP50 contains four putative CDK phosphorylation sites: Thr-5, Ser-176, Ser-264, and Ser-306 (Figure S4A). Consistent with MEP50 being a direct substrate, recombinant MEP50 was phosphorylated by cyclin D1/CDK4 and D1T286A/CDK4 in vitro (Figure 4B; Figure S4B). To identify phosphorylated residues, we phosphorylated recombinant MEP50 in vitro with purified cyclin D1T286A/CDK4 and subjected it to mass spectometry; we also affinity purified MEP50 from cells coexpressing cyclin D1T286A/CDK4 for the same analysis. Both approaches revealed phosphorylation of MEP50 at Thr-5 (Figures S4C–S4D). We generated recombinant MEP50 proteins harboring alanine substitutions at all four putative CDK phosphorylation sites and used these as substrates. Mutation of Thr-5 dramatically reduced phosphate incorporation; mutation of Ser-264 and Ser-306 also resulted in a moderate reduction, whereas Ser-176A had no apparent effect (Figure 4C).

If *CUL4* repression and CDT1 stabilization depends on MEP50 phosphorylation by cyclin D1T286A/CDK4, we reasoned that overexpression of key nonphosphorylatable MEP50 mutants should be inhibitory. Indeed, expression of myc-tagged MEP50-T5A and, to a lesser degree, MEP50-S264A interfered with cyclin D1T286A-dependent CDT1 stabilization and *CUL4* loss during S-phase (Figure 4D). Collectively, these results reveal that MEP50 is a CDK4 substrate and that phosphorylation of MEP50 predominantly on Thr-5 dominantly mediates downstream function.

Cyclin D1T286A/CDK4 Regulates PRMT5 Methyltransferase Activity via MEP50 Phosphorylation

To determine whether phosphorylation of MEP50 can directly regulate PRMT5 methyltransferase activity independently of association with high-molecular-weight chromatin remodeling complexes, we performed coupled in vitro kinase/methyltransferase reactions with purified recombinant PRMT5/MEP50 produced in Sf9 cells. PRMT5-dependent methyltransferase activity was increased following a kinase reaction with purified cyclin D1T286A/CDK4 (Figure 5A). Additionally, increased PRMT5/MEP50 SAM-dependent methyltransferase activity directed toward histone H4 was readily apparent following incubation of PRMT5/MEP50 complexes purified from HeLa cells with cyclin D1T286A/CDK4 and, to a lesser degree, with cyclin D1/CDK4 (Figure 5B). To evaluate the role of MEP50 phosphorylation, we expressed either wild-type MEP50 or mutant MEP50 alleles in cells treated with MEP50 siRNA. Expression of MEP50-T5A maintained basal methyltransferase activity in vitro but was refractory to the CDK4-dependent increase of PRMT5 activation (Figure 5C). Serine-264 to alanine substitution also attenuated the response to cyclin D1T286A/CDK4, whereas alanine

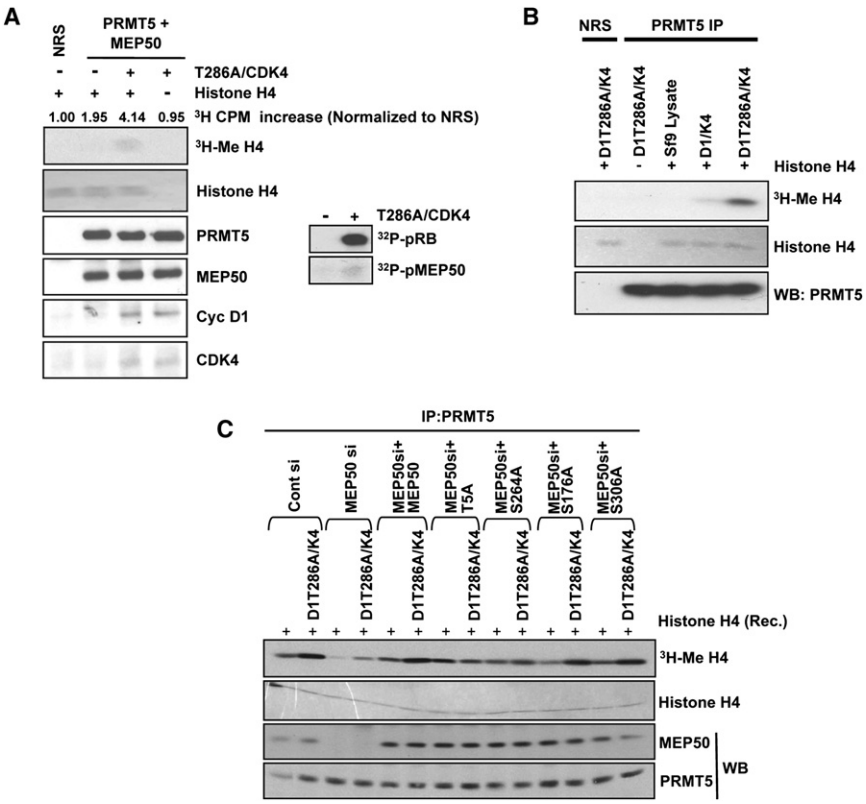

Figure 5. Cyclin D1T286A/CDK4 Increases PRMT5 Methyltransferase Activity through MEP50

(A and B) Purified cyclin D1/CDK4 and D1T286A/CDK4 kinases increase catalytic activity of PRMT5/MEP50 in vitro. Purified cyclin/CDK4 complexes from Sf9 cells were mixed with purified recombinant PRMT5/MEP50 produced in Sf9 cells (A) or PRMT5 complexes purified from HeLa cells (B) and incubated for 30 min with ATP at 30°C. PRMT5 complexes were washed and methyltransferase activity assessed using ^{3}H-Me (SAM) and recombinant Histone H4.

(C) Same as (B), except PRMT5 was purified from HeLa cells following MEP50 knockdown and re-expression of the indicated MEP50 mutants.

substitution at 176/306 was without influence. These results demonstrate that cyclin D1/CDK4 can increase histone methyltransferase activity of PRMT5/MEP50 through phosphorylation of Thr-5 and perhaps through Ser-264.

PRMT5/MEP50 Mediates Cyclin D1T286A-Dependent Rereplication, Transformation, and Survival of Cyclin D1T286A-Expressing Lymphoma Cells

Cyclin D1T286A/CDK4 expression induces rereplication in a CDT1-dependent fashion (Aggarwal et al., 2007). If PRMT5/MEP50 mediates rereplication, knockdown of PRMT5 should be inhibitory. Consistent with this hypothesis, we observed a dramatic reduction of >4N population from 26.8% to 2.28% with PRMT5 knockdown in T286A/CDK4/CDT1-transfected HeLa cells (Figures 6A and 6B).

We next determined whether PRMT5 mediates cyclin D1T286A-dependent transformation by knockdown of PRMT5 in murine fibroblasts, concurrent with expression of oncogenic RasV12 and cyclin D1T286A. Indeed, although cotransfection of both RasV12 and cyclin D1T286A induced focus formation (Figure 6C), foci number was reduced by 50% following knockdown of PRMT5. PRMT5 knockdown was not accompanied by cell cycle arrest (Figure S5A), suggesting that foci reduction is not a consequence of cell cycle arrest. In addition, PRMT5 knockdown did not significantly attenuate transformation mediated by Ras plus c-Myc, suggesting mechanistic specificity between PRMT5-dependent methyltransferase activity and constitutively nuclear cyclin D1 (Figure 6C).

To investigate therapeutic potential of targeting PRMT5, we determined whether inhibition of PRMT5 would compromise survival of primary Eμ-D1T286A lymphoma cells ex vivo. Because we were unable to efficiently introduce siRNA into these primary tumor cells, we utilized AMI-1. AMI-1 treatment increased death of tumor cells relative to normal controls (Figure 6D). In addition, treatment of primary lymphoma cells with MTA also triggered increased cell death relative to untreated tumor cells or MTA treated control lymphocytes (Figure S5B). Together, these observations suggest that PRMT5 plays an important role in promoting cyclin D1T286A/CDK4-dependent DNA rereplication, cell transformation, and survival of cells harboring constitutively active cyclin D1/CDK4.

To examine the role of MEP50 phosphorylation in cyclin D1T286A-dependent transformation, wild-type or phosphorylation-deficient T5A or S264A mutant MEP50 was coexpressed with RasV12 and cyclin D1T286A in NIH 3T3 cells. Compared to wild-type MEP50, expression of the T5A or S264A MEP50 mutant significantly reduced foci number, suggesting that phosphorylation of MEP50 and subsequent increase in PRMT5 activity is a driving force for cellular transformation in the presence of cyclin D1T286A (Figure 6E).

Fbx4 Inactivation Promotes Increased PRMT5-Dependent Histone Methylation

Although mutations directly targeting cyclin D1 do occur in human cancer (Benzeno et al., 2006), they occur infrequently relative to inactivation of the cyclin D1 E3 ligase (Barbash et al., 2008). Because inactivation of Fbx4 also drives nuclear accumulation of cyclin D1 kinase during S-phase, we postulated that Fbx4 loss should also impact PRMT5 function. We initially assessed this hypothesis in NIH 3T3 cells harboring Fbx4 shRNA (Lin et al., 2006). Fbx4 knockdown increased cyclin D1 and CDT1 and decreased CUL4A/B; critically, the level of H4R3 methylation was dramatically increased (Figure 7A). Previous work identified esophageal tumors harboring inactivating mutations in Fbx4 that resulted in strong cyclin D1 overexpression (Barbash

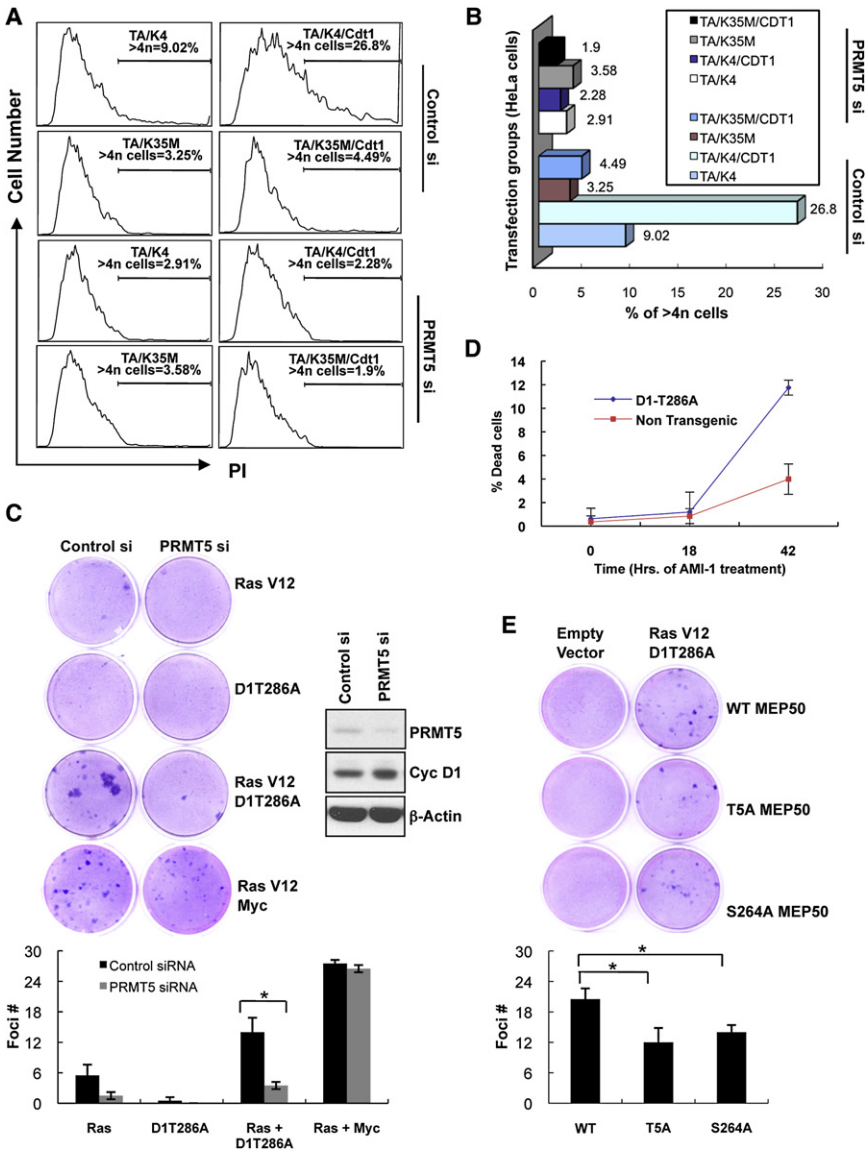

Figure 6. PRMT5 Knockdown Inhibits Cyclin D1T286A-Dependent DNA Rereplication, Cell Transformation, and Increases Death of Tumor Cells

(A) Following transfection of HeLa cells with the indicated expression plasmids, TA (D1T286A), K4 (CDK4), K35M (CDK4(K35M)), CDT1, cell cycle profile was assessed by FACS after PI staining.

(B) Graphical representation of the flow cytometry data from (A). The bars show the percentage of cells showing >4N DNA content.

(C) Foci formation assay was performed by concurrent knockdown of murine PRMT5 and overexpression of the indicated proteins in NIH 3T3 cells. Cells were grown for 14 days and stained with Giemsa to visualize foci. Quantification of data has been shown. Error bars represent standard deviation, and asterisk indicates $p < 0.05$.

(D) Single-cell suspensions of splenocytes prepared from nontransgenic or malignant Eμ-D1T286A transgenic tumor-burdened spleens were treated with 200 μM arginine methyltransferase inhibitor AMI-1. The cells were analyzed for the inhibitor sensitivity by measuring the percentage of cell death via AnnexinV –PI staining/flow cytometry. Values represent the mean of three independent experiments with error bars indicating ± SD .

(E) Foci formation assay was performed by transfection of the indicated MEP50 constructs along with empty vector control or RasV12 plus cyclin D1T286A in NIH 3T3 cells. Cells were grown for 14 days, and foci were analyzed as in (C). See also Figure S5.

DISCUSSION

Cyclin D1 is subject to intricate posttranslational control to ensure its temporal regulation. Cyclin D1 nuclear export followed by Fbx4-dependent ubiquitylation and degradation during S-phase are key features that serve to restrain nuclear cyclin D1/CDK4 activity and ensure normal cell division (Alt et al., 2000; Benzeno et al., 2006; Lin et al., 2006). Previous work revealed that aberrant nuclear accumulation of cyclin D1 during S-phase promotes transformation in vitro (Alt et al., 2000) and drives both B cell lymphomas and mammary carcinomas in mice (Gladden et al., 2006; Lin et al., 2008). Molecular analysis of these tumors revealed a potential mechanism wherein the cyclin D1-dependent kinase interferes with CUL4-dependent CDT1 proteolysis during S-phase (Higa et al., 2006; Sansam et al., 2006), because of transcriptional repression of *CUL4A* and *CUL4B*; the resulting overexpression of CDT1 during S-phase triggers DNA rereplication, enhancing genomic instability and the acquisition of fortuitous mutations (Aggarwal et al., 2007). A significant feature of the regulatory pathway leading to loss of *CUL4* expression is the noted dependence on cyclin D1/CDK4 activity. The current work revealing that phosphorylation of MEP50 on threonine 5 by cyclin D1T286A/CDK4 mediates PRMT5-dependent transcriptional

et al., 2008). We chose these same tumors to ascertain whether loss of Fbx4 function and overexpression of wild-type cyclin D1 kinase also correlated with increased H4R3 methylation. Immunohistochemical staining on tumor sections revealed a marked increase in H4R3 methylation relative to an esophageal tumor harboring wild-type Fbx4 or normal esophageal epithelium (Figure 7B). Because our analysis was restricted to tumors with known Fbx4 mutations and tissue availability for IHC (n = 4), our analysis did not achieve statistical significance. To support this analysis, we analyzed an esophageal tumor cell line harboring a mutant Fbx4, Fbx4(S8R) (TE10; Barbash et al., 2008) and another expressing both wild-type Fbx4 and cyclin D1 (TE15) and found that inactive Fbx4 correlates with increased CDT1 and methylated H4R3 (Figure 7C). Together, these observations demonstrate that stabilized nuclear cyclin D1 resulting from either cyclin D1 mutation or inactivation of Fbx4 results in increased PRMT5-dependent histone methylation.

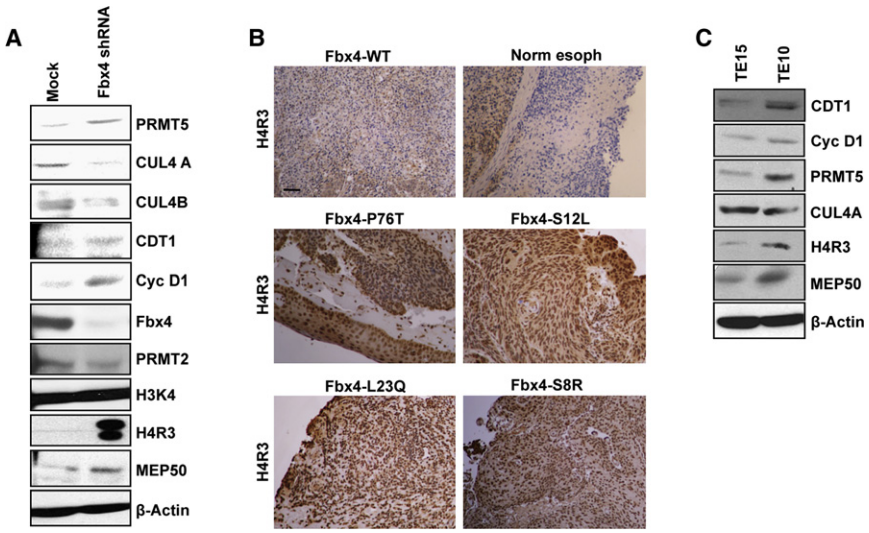

Figure 7. Knockdown of Fbx4 Stabilizes Nuclear Cyclin D1, Resulting in Increased PRMT5-Dependent Histone Methylation

(A) Direct western blot analysis of the protein lysates prepared from control NIH 3T3 or NIH 3T3 harboring Fbx4 knockdown.

(B) Representative immunohistochemistry images showing dimethyl H4R3 staining of human esophageal tumor sections. The scale bar represents 100 μm.

(C) Direct western blot analysis of the protein lysates prepared from TE15 and TE10 cell lines.

repression provides key mechanistic insights into the neoplastic activities of the cyclin D1/CDK4 enzyme.

Although PRMT5/MEP50 was identified through affinity purification of D1T286A complexes, it is the demonstration that MEP50 is a direct substrate for D-type cyclin dependent kinase that contributes a key advance in our understanding of cyclin D1-driven tumorigenesis. Phosphorylation of MEP50 on Thr-5 by D1T286A/CDK4 is necessary and sufficient to increase the intrinsic methyltransferase activity of PRMT5, resulting in increased H4R3/H3R8 methylation and repression of *CUL4A/B* expression. Notably, although we did not detect phosphorylation of Ser-264 in vivo, mutation of Ser-264 to alanine in MEP50 reduced cyclin D1-dependent induction of PRMT5 activity, suggesting that phosphorylation of this site may also contribute. The fact that inhibition of PRMT5/MEP50 activity by siRNA or overexpression of nonphosphorylatable MEP50 attenuates *CUL4* repression is consistent with a model in which PRMT5/MEP50 represents a key molecular target of nuclear cyclin D1/CDK4 during S-phase.

Regulation of PRMT5 by the Cyclin D1-Dependent Kinase

PRMT5 methylates arginines in multiple proteins, including myelin basic protein (Ghosh et al., 1988), SM proteins (Friesen et al., 2001), and p53 (Jansson et al., 2008). However, it is PRMT5-dependent histone dimethylation that is associated with transcriptional repression. Of the 11 PRMTs, PRMT5 is closely associated with transcriptional repression (Pal and Sif, 2007; Pal et al., 2004); its repressive function is attributed to symmetric dimethylation of histone 4 (arginine 3) and histone 3 (arginine 8) (Krause et al., 2007). These histone modifications were recently linked with the subsequent recruitment of DNMT3, linking histone methylation with DNA methylation (Zhao et al., 2009).

Regulation of PRMT5 function remains poorly understood and modification of PRMT5 by phosphorylation, acetylation, or ubiquitylation has not been reported. In contrast, association of PRMT5 with MEP50 is an activating event (Krause et al., 2007). In addition, association of COPR5 with PRMT5 changes the balance of activity from H3R8 toward H4R3 (Lacroix et al., 2008). Although PRMT5 is not detectably modified in a CDK4-dependent manner, a multiplicity of approaches revealed MEP50 to be a direct substrate. The data provided demonstrate that phosphorylation of Thr-5, and perhaps Ser-264, of MEP50 contributes to increased PRMT5/MEP50 methyltransferase activity in cells harboring nuclear cyclin D1/CDK4. Because addition of purified MEP50 to recombinant PRMT5 is sufficient to activate PRMT5 methyltransferase function (Krause et al., 2007), the most direct model is that cyclin D1-dependent phosphorylation functions as a switch to facilitate MEP50-dependent, structural alterations in PRMT5 that contribute to enhanced catalysis or perhaps increased affinity for substrates, which translates into more efficient methylation.

Transcriptional Regulation of *CUL4A/B* by Cyclin D1

Previous work demonstrated that nuclear, active cyclin D1/CDK4 during S-phase leads to reduced *CUL4A/B* expression (Aggarwal et al., 2007). Although the underlying mechanism remained elusive, a large body of work associating cyclin D1 with transcriptional regulation suggested that regulation could be direct. For example, cyclin D1 was first noted to associate with the estrogen receptor (ER) to coordinate ligand-independent expression of ER targets independent of CDK activation (Lamb et al., 2000; McMahon et al., 1999; Zwijsen et al., 1998; Zwijsen et al., 1997). Subsequently, cyclin D1 was shown to bind and regulate the activities of androgen receptor (Knudsen et al., 1999), DMP1 (Hirai and Sherr, 1996), and C/EBPβ (Lamb et al., 2003). Our current work demonstrates that regulation reflects CDK4-dependent phosphorylation of MEP50, which, in turn, increases PRMT5-dependent histone methylation of target genes, reducing their expression. Although previous work supports a model in which cyclin D1 functions as a molecular bridge between DNA-bound transcription factors and coactivators or repressors, our data reveal not only that cyclin D1 occupies promoter regions of a target gene, but also that regulation reflects CDK-dependent phosphorylation of a recruited epigenetic regulatory enzyme. Consistently, recent work utilizing genome-wide ChIP analysis demonstrated that cyclin D1 is enriched in regions near the transcriptional start site of a large number of genes (Bienvenu et al., 2010), providing additional

evidence for cyclin D1 directly regulating gene expression. It is intriguing to note that the strongest H4R3 methylation occurs near the predicted transcription start site of both *CUL4A* and *CUL4B*.

The role of CDK4, although perhaps unexpected in the context of transcription, is not totally unexpected in the context of tumorigenesis given that CDK activation is central to the function of cyclin D1 during neoplastic transformation. That MEP50 is a substrate for cyclin D1/CDK4 makes the PRMT5/MEP50 complex one of a limited number of cyclin D1-dependent substrates. Previously, only the RB family members (Kato et al., 1993) and Smad3, a key mediator for TGF-β antiproliferative responses (Liu and Matsuura, 2005; Matsuura et al., 2004), have been established as substrates in vitro and in vivo.

Although increased cyclin D1T286A/CDK4-dependent PRMT5/MEP50 function is required for *CUL4* loss and CDT1 overexpression, we cannot rule out the contribution of additional mechanisms that contribute to *CUL4* regulation. For example, neither cyclin D1 nor PRMT5/MEP50 has intrinsic DNA-binding properties. Thus, it remains unclear how cyclin D1T286A/CDK4 promotes the targeting to this locus. In addition, we questioned the possibility that cyclin D1T286A might result in the recruitment of histone deacetylases and thereby impact *CUL4* expression. Our results indicated that HDAC inhibition resulted in increased *CUL4* expression regardless of cyclin D1T286A/CDK4, suggesting a nonspecific effect (Figures S2G and S2H).

Signaling Through PRMT5/MEP50 Is Not Limited to Lymphoid Tumors Harboring Mutant Cyclin D1 Alleles

Cyclin D1T286A/CDK4 increases PRMT5 methyltransferase activity in vivo through MEP50, revealing a pathway whereby PRMT5 facilitates cyclin D1T286A/CDK4-dependent rereplication and survival of murine tumors harboring a lymphoid-specific D1T286A transgene. However, it is important to note that this mechanism is not restricted to this model system or this particular cyclin D1 allele for the following reasons. First, knockdown of Fbx4, the specificity component of the cyclin D1 E3 ligase, stabilizes nuclear cyclin D1/CDK4 complexes in the nucleus during S-phase and thereby increases PRMT5-dependent histone methylation, resulting in *CUL4* loss. Second, human tumors harboring inactivating mutations in Fbx4 and subsequent nuclear accumulation of endogenous cyclin D1-dependent kinase, exhibit a dramatic increase in H4R3 methylation. Finally, cyclin D1/CDK4-MEP50/PRMT5 complexes are observed in esophageal carcinoma cell lines harboring cyclin D1P287A. These independent findings implicate aberrant nuclear cyclin D1 in transcriptional repression of *CUL4.*

Collectively, our current work supports a model wherein accumulation of nuclear cyclin D1/CDK4 during S-phase triggers increased PRMT5/MEP50 activity, thereby specifically reducing *CUL4* expression (and triggering downstream stabilization of CUL4 ligase targets such as CDT1). Our functional analysis revealed that PRMT5 is necessary for cyclin D1-mediated cell transformation and further that tumors harboring dysregulated cyclin D1 exhibit increased PRMT5-dependent histone methylation. Future efforts to determine the global gene expression pattern altered through cyclin D1-dependent regulation of PRMT5 and which of these specifically contribute to neoplastic growth will be of significant importance.

EXPERIMENTAL PROCEDURES

Cell Culture, Transfections, and Plasmids

Cell culture conditions and transfections were performed as previously noted (Aggarwal et al., 2007). The human PRMT5 Myc-tagged vector was generated by PCR using primers designed for directional cloning into pCS2-MT plasmid (in frame with six Myc epitope tags at the N terminus of PRMT5), using PRMT5 cDNA (Open Biosystems) as the template. Human GST-tagged MEP50 vector was generated by PCR of human MEP50 with primers designed for directional cloning into pGEX-4T-1 plasmid (in frame with GST tag at the N terminus of MEP50), using pOTB7-MEP50 (Open Biosystems) as the template. Human MEP50 Myc-tagged vector was generated by PCR of human MEP50 with primers designed for directional cloning into pcDNA3 plasmid (in frame with 1X Myc tag at the N terminus of MEP50). Site-directed mutagenesis was performed with QuikChange Site-Directed Mutagenesis Kit (Stratagene) according to the manufacturer's instructions. All clones were sequenced in their entirety.

Chromatin Immunoprecipitation Assay

For ChIP, cells were cross-linked in 0.75% formaldehyde for 10 min and quenched with 0.18 mM glycine for 5 min. Cells were harvested in cell lysis buffer (50 mM HEPES [pH 7.5], 140 mM NaCl, 1 mM EDTA [pH 8.0], 1.0% Triton X-100, 0.1% SDS, 0.1% deoxycholate, and fresh protease inhibitors) and chromatin sheared to an average size of 350–600 bp by sonication (3 × 10min cycles of 30 × 30 s each) at constant output on high setting (Bioruptor). Sonicated DNA was diluted 3-fold in dilution buffer (20 mM Tris-HCl [pH 8.0], 2mM EDTA [pH 8.0], 1% Triton X-100, 150 mM NaCl, and protease inhibitors) and was precleared with protein A plus agarose (Millipore). Lysates were rotated at 4°C overnight with 5 μg of polyclonal antibodies specific for H4R3 (Abcam) or H3R8 anti-sera, as described below, including PRMT5 (Abcam), M2 monoclonal, (Sigma), Brg1 (Santa Cruz), or normal rabbit IgG (Cell Signaling). After washing, complexes were eluted in 130 μl of elution buffer (1% SDS plus 100 mM $NaHCO_3$), followed by addition of 100 μg of proteinase K at 65°C overnight for crosslink reversal. The DNA was purified by phenol-chloroform extraction, and precipitated DNA was analyzed by qPCR. The primers used for *CUL4A* and *CUL4B* have been described in Figure S3D.

Immunoprecipitation and Immunoblot Analysis

Cells were harvested in Tween-20 buffer (50 mM HEPES [pH 8.0], 150 mM NaCl, 2.5 mM EGTA, 1 mM EDTA, and 0.1% Tween 20), protease, and phosphatase inhibitors (1 mM PMSF, 20 U/ml aprotinin, 5 μg/ml leupeptin, 1 mM DTT, 0.4 μM NaF, and 10 μM β-glycerophosphate), and protein concentration of samples was determined by BCA assay. Cyclin D1, PRMT5, and MEP50 were precipitated using M2 anti-flag agarose (to recognize flag-tagged proteins; Sigma-Aldrich), PRMT5 rabbit polyclonal antibody (Abcam), or c-*myc* (9E10) and MEP50 rabbit polyclonal antibody (Bethyl Lab), respectively. Proteins were resolved by SDS-PAGE, transferred to nitrocellulose membranes, and analyzed by immunoblotting. Antibodies used in these studies were as follows: Fbx4 rabbit polyclonal antibody (Rockland Immunochemicals); cyclin D1 mouse monoclonal antibody D1-72-13G and cyclin D1 mouse anti-human (Calbiochem); β-actin mouse monoclonal (Sigma-Aldrich); Cul4A rabbit polyclonal (Bethyl Lab. Inc); Cul4B rabbit polyclonal (ProteinTech Group Inc); pSP/TP mouse monoclonal (16B4, Biomol); CDK4 (C-22 or H-22), Cdt1, Brg1, RB, PRMT5 mouse monoclonal, PRMT2, and mSin3a (Santa Cruz); and H4R3 rabbit polyclonal-ChIP grade, H3K4 rabbit polyclonal, Histone H3 rabbit polyclonal, PRMT1 and PRMT7, and Histone H4 rabbit polyclonal (Abcam). Anti-H3R8 (corresponding to symmetric dimethylated R8 of human histone H3) antibody was generated by immunizing rabbits with peptide containing modified histone H3 (YenZym Antibodies, LLC) and subsequent affinity purification. Antibody binding was visualized by chemiluminescence (Perkin Elmer). Figures S3A–S3C reveal the specificity of this antibody.

Immunohistochemistry

Human esophageal tumors harboring Fbx4 mutations and normal esophageal tissue were obtained with informed consent and with Institutional Review Board approval from the University of Pennsylvania (IRB #803902), Fox Chase Cancer Center (IRB #98-53), and University of Fukui, Japan (IRB #H190228-155). Tissue was fixed in 10% buffered formalin and subsequently was

dehydrated, paraffin embedded, and sectioned. Tissue sections were immunostained as described previously (Aggarwal et al., 2007), with rabbit polyclonal H4R3 (Abcam) at 1:500 dilution as the primary antibody.

In Vitro Kinase Assay and In Vitro Methyltransferase Assay

Purified GST-MEP50 wild-type, GST-T5A, S176A, S264A, S306A mutants, and GST-RB were used as substrates for in vitro kinase reactions (Matsushime et al., 1994). Cyclin D1/CDK4 kinase complexes were purified from Sf9 cells. For assessment of PRMT5 methyltransferase activity, PRMT5 complexes were collected from the indicated sources by immune precipitation. Beads were washed in Tween-20 buffer followed by methyltransferase buffer (15 mM HEPES [pH 7.9], 100 mM KCl, 5 mM $MgCl_2$, 20% Glycerol, 1 mM EDTA, 0.25 mM DTT, and 0.5 mM PMSF). The methylation reaction included PRMT5 immune complexes on beads, 1 μg recombinant Histone H4 (NEB), and 2.75 μCi S-adenosyl-L-(methyl-^{3}H)methionine (Amersham Pharmacia) in a total volume of 25 μl for 1.5 hr at 30°C. The reaction mixture was resolved on a SDS-polyacrylamide gel, and modified histone H4 was detected by fluorography. For the coupled kinase assay/methyltransferase assay, cyclin complexes were purified from Sf9 cells and mixed with purified recombinant PRMT5/MEP50 complex (produced in Sf9 cells, BPS Bioscience) or PRMT5 immune precipitated from HeLa cells immobilized on beads. In vitro kinase assays were performed for 30 min at 30°C in kinase buffer. PRMT5-containing beads were washed into methyltransferase buffer, followed by in vitro methylation reaction for 2 hr at 30°C with 2 μg H4 substrate and 2.75 μCi ^{3}H-SAM. Methylated H4 was visualized by fluorography or scintillation counting for ^{3}H incorporation.

Foci Formation

Low passage NIH 3T3 cells were transfected with control or murine PRMT5 siRNA (Dharmacon) with HiPerfect (QIAGEN). Twenty-four hours after siRNA delivery, cells were transfected with 2 μg of the indicated plasmids (pBabe Ras V12 or pBabe cyclin D1T286A) or empty vector (pBabe puro) using Lipofectamine/Plus Reagent (Invitrogen). Transfected cells were counted after 48 hr, and 2×10^5 cells were plated in duplicate on 35 mm plates in DMEM containing 5% FBS. Cells were re-fed with DMEM plus 5% FBS every 2 days for 14 days, followed by staining with Giemsa to visualize foci formation. Foci were counted for duplicate plates; in the figures, error bars represent ± standard deviation and asterisks indicate $p < 0.05$, as determined by Student's t test. For MEP50 overexpression assays, NIH 3T3 cells were transfected with 2 μg of wild-type MEP50 or phosphorylation-deficient MEP50 mutant T5A or S264A, along with empty vector or Ras V12 and cyclin D1T286A constructs, as indicated. Cells were seeded and foci formation was analyzed as described above.

Real-Time Quantitative PCR Analysis of Gene Expression

RNA isolation was performed using standard protocols. DNA fragments were generated by reverse transcriptase PCR (RT-PCR; Superscript™, Invitrogen). Mixed primer/probe sets for human *CUL4A/B* and 18S rRNA were used to measure the levels of these transcripts using the Applied Biosystems 7900HT sequence detection system, in accordance with the manufacturer's instructions. Primers used for detection of human *CUL4A* and *CUL4B* were described previously (Aggarwal et al., 2007).

siRNA and Methyltransferase Inhibitor Experiments

siGENOME SMARTpool targeting PRMT5 and MEP50 or control siRNA were purchased from Dharmacon. HeLa cells were treated with indicated siRNA or methyltransferase inhibitors, MTA (Sigma) or AMI-1 (Calbiochem), for 24 hr followed by transfection and synchronization of cells in G1 and S-phases. For targeting 3′ UTR region of human MEP50, siRNA (5′-CUCCUUACCA UUAAACUGA-3′) was designed and purchased from Sigma.

SUPPLEMENTAL INFORMATION

Supplemental information includes one table and five figures and can be found with this article online at doi:10.1016/j.ccr.2010.08.012.

ACKNOWLEDGMENTS

The authors wish to thank Margarita Romero for excellent technical assistance and Chao Lu for assistance in profiling the H3R8 antibody. This work was supported by grants from the National Institutes of Health (CA93237) and a Leukemia & Lymphoma Scholar award (to J.A.D.); P01-CA098101 (to A.K.R., M.H., and J.A.D.); CA090465, CA098172; and funds from the Commonwealth Universal Research Enhancement Program, Pennsylvania Department of Health (to S.B.M.). Support was also provided by the Morphology Core Facility (S. Mitchell).

Received: February 23, 2010
Revised: May 13, 2010
Accepted: August 12, 2010
Published: October 18, 2010

REFERENCES

Aggarwal, P., Lessie, M.D., Lin, D.I., Pontano, L., Gladden, A.B., Nuskey, B., Goradia, A., Wasik, M.A., Klein-Szanto, A.J., Rustgi, A.K., et al. (2007). Nuclear accumulation of cyclin D1 during S phase inhibits Cul4-dependent Cdt1 proteolysis and triggers p53-dependent DNA rereplication. Genes Dev. *21*, 2908–2922.

Alt, J.R., Cleveland, J.L., Hannink, M., and Diehl, J.A. (2000). Phosphorylation-dependent regulation of cyclin D1 nuclear export and cyclin D1-dependent cellular transformation. Genes Dev. *14*, 3102–3114.

Bani-Hani, K., Martin, I.G., Hardie, L.J., Mapstone, N., Briggs, J.A., Forman, D., and Wild, C.P. (2000). Prospective study of cyclin D1 overexpression in Barrett's esophagus: association with increased risk of adenocarcinoma. J. Natl. Cancer Inst. *92*, 1316–1321.

Barbash, O., Zamfirova, P., Lin, D.I., Chen, X., Yang, K., Nakagawa, H., Lu, F., Rustgi, A.K., and Diehl, J.A. (2008). Mutations in Fbx4 inhibit dimerization of the SCF(Fbx4) ligase and contribute to cyclin D1 overexpression in human cancer. Cancer Cell *14*, 68–78.

Bartkova, J., Lukas, J., Muller, H., Lutzhoft, D., Strauss, M., and Bartek, J. (1994a). Cyclin D1 protein expression and function in human breast cancer. Int. J. Cancer *57*, 353–361.

Bartkova, J., Lukas, J., Muller, H., Strauss, M., Gusterson, B., and Bartek, J. (1995). Abnormal patterns of D-type cyclin expression and G1 regulation in human head and neck cancer. Cancer Res. *55*, 949–956.

Bartkova, J., Lukas, J., Strauss, M., and Bartek, J. (1994b). The PRAD-1/cyclin D1 oncogene product accumulates aberrantly in a subset of colorectal carcinomas. Int. J. Cancer *58*, 568–573.

Benzeno, S., Lu, F., Guo, M., Barbash, O., Zhang, F., Herman, J.G., Klein, P.S., Rustgi, A., and Diehl, J.A. (2006). Identification of mutations that disrupt phosphorylation-dependent nuclear export of cyclin D1. Oncogene *25*, 6291–6303.

Bienvenu, F., Jirawatnotai, S., Elias, J.E., Meyer, C.A., Mizeracka, K., Marson, A., Frampton, G.M., Cole, M.F., Odom, D.T., Odajima, J., et al. (2010). Transcriptional role of cyclin D1 in development revealed by a genetic-proteomic screen. Nature *463*, 374–378.

Cheng, D., Yadav, N., King, R.W., Swanson, M.S., Weinstein, E.J., and Bedford, M.T. (2004). Small molecule regulators of protein arginine methyltransferases. J. Biol. Chem. *279*, 23892–23899.

Diehl, J.A. (2002). Cycling to cancer with cyclin Dl. Cancer Biol. Ther. *1*, 226–231.

Friesen, W.J., Paushkin, S., Wyce, A., Massenet, S., Pesiridis, G.S., Van Duyne, G., Rappsilber, J., Mann, M., and Dreyfuss, G. (2001). The methylosome, a 20S complex containing JBP1 and pICln, produces dimethylarginine-modified Sm proteins. Mol. Cell. Biol. *21*, 8289–8300.

Ghosh, S.K., Paik, W.K., and Kim, S. (1988). Purification and molecular identification of two protein methylases I from calf brain: Myelin basic protein- and histone-specific enzyme. J. Biol. Chem. *263*, 19024–19033.

Gillett, C., Fantl, V., Smith, R., Fisher, C., Bartek, J., Dickson, C., Barnes, D., and Peters, G. (1994). Amplification and overexpression of cyclin D1 in breast

cancer detected by immunohistochemical staining. Cancer Res. *54*, 1812–1817.

Gladden, A.B., Woolery, R., Aggarwal, P., Wasik, M.A., and Diehl, J.A. (2006). Expression of constitutively nuclear cyclin D1 in murine lymphocytes induces B-cell lymphoma. Oncogene *25*, 998–1007.

Herman, J.G., Merlo, A., Mao, L., Lapidus, R.G., Issa, J.P., Davidson, N.E., Sidransky, D., and Baylin, S.B. (1995). Inactivation of the CDKN2/p16/MTS1 gene is frequently associated with aberrant DNA methylation in all common human cancers. Cancer Res. *55*, 4525–4530.

Hibberts, N.A., Simpson, D.J., Bicknell, J.E., Broome, J.C., Hoban, P.R., Clayton, R.N., and Farrell, W.E. (1999). Analysis of cyclin D1 (CCND1) allelic imbalance and overexpression in sporadic human pituitary tumors. Clin. Cancer Res. *5*, 2133–2139.

Higa, L.A., Banks, D., Wu, M., Kobayashi, R., Sun, H., and Zhang, H. (2006). L2DTL/CDT2 interacts with the CUL4/DDB1 complex and PCNA and regulates CDT1 proteolysis in response to DNA damage. Cell Cycle *5*, 1675–1680.

Hirai, H., and Sherr, C.J. (1996). Interaction of D-type cyclins with a novel myb-like transcription factor, DMP1. Mol. Cell. Biol. *16*, 6457–6467.

Hosokawa, Y., and Arnold, A. (1998). Mechanism of cyclin D1 (CCND1, PRAD1) overexpression in human cancer cells: analysis of allele-specific expression. Genes Chromosomes Cancer *22*, 66–71.

Hosokawa, Y., Joh, T., Maeda, Y., Arnold, A., and Seto, M. (1999). Cyclin D1/PRAD1/BCL-1 alternative transcript [B] protein product in B-lymphoid malignancies with t(11;14)(q13;q32) translocation. Int. J. Cancer *81*, 616–619.

Hou, Z., Peng, H., Ayyanathan, K., Yan, K.P., Langer, E.M., Longmore, G.D., and Rauscher, F.J., 3rd. (2008). The LIM protein AJUBA recruits protein arginine methyltransferase 5 to mediate SNAIL-dependent transcriptional repression. Mol. Cell. Biol. *28*, 3198–3207.

Iwasaki, H., and Yada, T. (2007). Protein arginine methylation regulates insulin signaling in L6 skeletal muscle cells. Biochem. Biophys. Res. Commun. *364*, 1015–1021.

Jansson, M., Durant, S.T., Cho, E.C., Sheahan, S., Edelmann, M., Kessler, B., and La Thangue, N.B. (2008). Arginine methylation regulates the p53 response. Nat. Cell Biol. *10*, 1431–1439.

Jin, M., Inoue, S., Umemura, T., Moriya, J., Arakawa, M., Nagashima, K., and Kato, H. (2001). Cyclin D1, p16 and retinoblastoma gene product expression as a predictor for prognosis in non-small cell lung cancer at stages I and II. Lung Cancer *34*, 207–218.

Kato, J., Matsushime, H., Hiebert, S.W., Ewen, M.E., and Sherr, C.J. (1993). Direct binding of cyclin D to the retinoblastoma gene product (pRB) and pRB phosphorylation by the cyclin D-dependent kinase CDK4. Genes Dev. *7*, 331–342.

Knudsen, K.E., Cavenee, W.K., and Arden, K.C. (1999). D-type cyclins complex with the androgen receptor and inhibit its transcriptional transactivation ability. Cancer Res. *59*, 2297–2301.

Krause, C.D., Yang, Z.H., Kim, Y.S., Lee, J.H., Cook, J.R., and Pestka, S. (2007). Protein arginine methyltransferases: evolution and assessment of their pharmacological and therapeutic potential. Pharmacol. Ther. *113*, 50–87.

Lacroix, M., Messaoudi, S.E., Rodier, G., Le Cam, A., Sardet, C., and Fabbrizio, E. (2008). The histone-binding protein COPR5 is required for nuclear functions of the protein arginine methyltransferase PRMT5. EMBO Rep. *9*, 452–458.

Lamb, J., Ladha, M.H., McMahon, C., Sutherland, R.L., and Ewen, M.E. (2000). Regulation of the functional interaction between cyclin D1 and the estrogen receptor. Mol. Cell. Biol. *20*, 8667–8675.

Lamb, J., Ramaswamy, S., Ford, H.L., Contreras, B., Martinez, R.V., Kittrell, F.S., Zahnow, C.A., Patterson, N., Golub, T.R., and Ewen, M.E. (2003). A mechanism of cyclin D1 action encoded in the patterns of gene expression in human cancer. Cell *114*, 323–334.

Lin, D.I., Barbash, O., Kumar, K.G., Weber, J.D., Harper, J.W., Klein-Szanto, A.J., Rustgi, A., Fuchs, S.Y., and Diehl, J.A. (2006). Phosphorylation-dependent ubiquitination of cyclin D1 by the SCF(FBX4-alphaB crystallin) complex. Mol. Cell *24*, 355–366.

Lin, D.I., Lessie, M.D., Gladden, A.B., Bassing, C.H., Wagner, K.U., and Diehl, J.A. (2008). Disruption of cyclin D1 nuclear export and proteolysis accelerates mammary carcinogenesis. Oncogene *27*, 1231–1242.

Liu, F., and Matsuura, I. (2005). Inhibition of Smad antiproliferative function by CDK phosphorylation. Cell Cycle *4*, 63–66.

Lu, F., Gladden, A.B., and Diehl, J.A. (2003). An alternatively spliced cyclin D1 isoform, cyclin D1b, is a nuclear oncogene. Cancer Res. *63*, 7056–7061.

Matsushime, H., Quelle, D.E., Shurtleff, S.A., Shibuya, M., Sherr, C.J., and Kato, J.Y. (1994). D-type cyclin-dependent kinase activity in mammalian cells. Mol. Cell. Biol. *14*, 2066–2076.

Matsuura, I., Denissova, N.G., Wang, G., He, D., Long, J., and Liu, F. (2004). Cyclin-dependent kinases regulate the antiproliferative function of Smads. Nature *430*, 226–231.

McMahon, C., Suthiphongchai, T., DiRenzo, J., and Ewen, M.E. (1999). P/CAF associates with cyclin D1 and potentiates its activation of the estrogen receptor. Proc. Natl. Acad. Sci. USA *96*, 5382–5387.

Pal, S., and Sif, S. (2007). Interplay between chromatin remodelers and protein arginine methyltransferases. J. Cell. Physiol. *213*, 306–315.

Pal, S., Vishwanath, S.N., Erdjument-Bromage, H., Tempst, P., and Sif, S. (2004). Human SWI/SNF-associated PRMT5 methylates histone H3 arginine 8 and negatively regulates expression of ST7 and NM23 tumor suppressor genes. Mol. Cell. Biol. *24*, 9630–9645.

Sansam, C.L., Shepard, J.L., Lai, K., Ianari, A., Danielian, P.S., Amsterdam, A., Hopkins, N., and Lees, J.A. (2006). DTL/CDT2 is essential for both CDT1 regulation and the early G2/M checkpoint. Genes Dev. *20*, 3117–3129.

Zhao, Q., Rank, G., Tan, Y.T., Li, H., Moritz, R.L., Simpson, R.J., Cerruti, L., Curtis, D.J., Patel, D.J., Allis, C.D., et al. (2009). PRMT5-mediated methylation of histone H4R3 recruits DNMT3A, coupling histone and DNA methylation in gene silencing. Nat. Struct. Mol. Biol. *16*, 304–311.

Zwijsen, R.M., Buckle, R.S., Hijmans, E.M., Loomans, C.J., and Bernards, R. (1998). Ligand-independent recruitment of steroid receptor coactivators to estrogen receptor by cyclin D1. Genes Dev. *12*, 3488–3498.

Zwijsen, R.M., Wientjens, E., Klompmaker, R., van der Sman, J., Bernards, R., and Michalides, R.J. (1997). CDK-independent activation of estrogen receptor by cyclin D1. Cell *88*, 405–415.